BookID 186658_ChapID 4_Proof# 1 - 17/02/10

4

The Effect of Morphology of Activated Electrodes on Their Electrochemical Activity

Konstantin I. Popov,[1,2] Predrag M. Živković,[2] and Nebojša D. Nikolić[1]

[1] *ICTM-Institute of Electrochemistry, University of Belgrade, Njegoševa 12, Belgrade, Serbia*
[2] *Faculty of Technology and Metallurgy, University of Belgrade, Karnegijeva 4, Belgrade, Serbia*

I. INTRODUCTION

The noble metals or their oxides are the most convenient substrates for most electrochemical reactions taking place in fuel cells or in industrial electrolysis, for example. Because of this, the "activated" electrodes are introduced, consisting of a conducting, inert support coated with a thin layer of electrocatalyst. In this way, not only the chemical nature of the electrode can be modified but also its morphology and structure in dependence on the procedure of preparation.[1]

The transformation of the properties of an electrode surface from those of an inexpensive inert substrate to those of an active one with a small quantity of an expensive active metal is one of the most important problems of electrocatalysis today. Numerous papers substantiate that different catalyst for different electrochemical

S.S. Djokić (ed.), *Electrodeposition: Theory and Practice*,
Modern Aspects of Electrochemistry 48, DOI 10.1007/978-1-4419-5589-0_4,

reactions have been developed by placing appropriate active nanoparticles, usually of noble metals, on a carbon support, for example, for the electrochemical oxidation of methanol,[2] the electrochemical reduction of oxygen,[3] the electrochemical oxidation of oxalic acid,[4] etc. Naturally, the catalyst can also be placed on metal or carbon substrate by electrodeposition. Formerly, metallic supports were the only substrates used in cathodic formation of electrodeposits. Nowadays, various exotic conductive materials are also experimented.[5]

According to Bockris et al.,[6] the cell voltage of a self-driving cell, U_s, is given by

$$U_s = U_e - \Delta U \tag{1}$$

and the cell voltage of a driven cell, U_d, by

$$U_d = U_e + \Delta U. \tag{2}$$

The power P_s, which can be obtained from self-driving cells, like batteries and fuel cells, is

$$P_s = (U_e - \Delta U)I \tag{3}$$

and the power P_d, required for driving the cells in, for example, electrowining of metals, is

$$P_d = (U_e + \Delta U)I, \tag{4}$$

where

$$\Delta U = \eta_a + \eta_c + IR \tag{5}$$

and U_e is the equilibrium cell potential, η_a and η_c the absolute values of overpotentials of both electrodes, and I and R are the cell current and cell Ohmic resistance, respectively.

The overpotential η in mixed activation–diffusion control is given by

$$\eta = \eta_{ac} + \eta_d, \tag{6}$$

where η_{ac} and η_d are the activation and diffusion overpotential, respectively. It follows from (3) to (6) that ΔU, P_s, and P_d depend on both activation and diffusion overpotentials and on Ohmic voltage drop in the cell.

The activation overpotential mainly depends on the kinetic parameters of processes under consideration on the given substrate

and on the actual current density. The diffusion overpotential mainly depends on the actual current density to the limiting current density ratio, and the Ohmic voltage drop depends on the current in the cell, the composition of the solution, and geometry of the system. AQ1

Obviously, ΔU represents the losses of energy, and making U near U_e, or ΔU as low as possible, is the crucial problem of the applied electrochemistry.

There are two basic problems in activation of inert substrates by electrodeposition: first, the effect of the structure of the active surface film on the transformation of electrode from inert to active one[7] and second, effect of the surface morphology on the polarization characteristics of activated electrodes.[8,9] Obviously, in the last case, the nature of the initial substrate is not important. The analysis of both of them is the aim of this chapter. It will be performed for the cathodic reactions. Obviously, the corresponding analysis for the anodic processes can be performed in the similar way.

Metallic electrodeposits allow surfaces with a variety of morphological characteristics to be obtained. The granular electrodeposits represent the model of the partially covered inert substrate.[7] Deposits with a high roughness factor and good mechanical resistance are of particular interest. These two important aspects are usually mutually exclusive, as high values of the roughness factor are mainly obtained through growth of dendrites that have low mechanical resistance.[10] Hence, such coverings are unsuitable as electrocatalysts. On the other hand, the dendritic deposits are the best-known form of the disperse deposits,[11–13] being the most suitable for theoretical analysis. The dendrites are used here as an example of the disperse deposit characterized with large roughness factor during the analysis of the polarization behavior of activated electrodes. This is because this chapter is written in order to explain the polarization behavior of activated electrodes, not to give some concrete technical solutions.

II. MICRO- AND MACROELECTRODES

In all actual electrochemical converters, the electrodes are three-dimensional, porous structures, the pores of which contain the catalyst material to and from which electric charge transfer occurs.[14]

The electrodic catalyst consists of active nanoparticles. The distribution of the active material on the surface inside the pores is very

important for obtaining the necessary activity of the solid phase. This is because the activity of a porous structure depends on both mass transfer through it and on the electrochemical properties of the surface.[7]

Mass transfer in a porous structure strongly depends on macrogeometric parameters, but the electrochemical properties of the surface of the solid phase depend on the mutual relation of the active particles on it, being independent of the macrogeometry of the system.

In spite of some specific characteristics of nanoparticles, this can also be treated as the case of an inert substrate modified with active grains in general. Naturally, for the sake of simplicity, this analysis can be performed for planar electrodes.

According to Scharifker and Hills,[15] in systems where the charge transfer is fast, the rates of growth of nuclei are well described in terms of control by mass transfer of the electrodepositing ions to the growth centers.

During this stage of the growth of the deposit, the nuclei develop diffusion zones around themselves, and as these zones overlap, the hemispherical mass transfer gives way to linear mass transfer to an effectively planar surface. The current then falls, and the transient approaches that corresponding to the total electrode surface.

Similarly, it was shown by Gilleadi[16] that the development of a diffusion field near the surface of an ensemble of microelectrodes occurs in the four successive steps, assuming total diffusion control of the process. The ensemble of microelectrodes consists of microelectrodes placed on the inert surface at distances between their centers larger than their diameter. The first, planar diffusion to the microelectrodes; the second, spherical diffusion with no overlap; the third, spherical diffusion with substantial overlap; and finally, total overlap, equivalent to planar diffusion to the whole surface.

Stonehart and Wheeler[17] and Popov et al.[7] correlated the current densities on the microelectrodes, taking into account the change of concentration around them, with the current density on the macroelectrode. This is because the charge transfer occurs on the microelectrodes, while the mass-transfer limitations are related to the diffusion layer of the macroelectrode. In this chapter, the model of the surface of Popov et al.[7] will be used to describe the polarization behavior of previously activated inert macroelectrode with active microelectrodes.

The cathodic polarization curve equation for flat or large spherical electrode is given by

$$j = \frac{j_0(f_c - f_a)}{1 + \frac{j_0 f_c}{j_L}}, \tag{7}$$

where j, j_0, and j_L are the current density, exchange current density, and limiting diffusion current density, respectively, and

$$f_c = 10^{\frac{\eta}{b_c}}, \tag{8}$$

$$f_a = 10^{-\frac{\eta}{b_a}}, \tag{9}$$

where b_c and b_a are the cathodic and anodic Tafel slopes and η is the overpotential. Equation (7) is modified for use in electrodeposition of metals by taking cathodic current density and overpotential as positive. Derivation of (7) is performed under assumption that the concentration dependence of j_0 can be neglected.[12,18,19]

It is known[12] that electrochemical processes on microelectrodes in bulk solution can be under activation control at overpotentials, which correspond to the limiting diffusion current density plateau of the macroelectrode. The cathodic limiting diffusion current density, $j_{L,Sp}$, for steady-state spherical diffusion is given by:

$$j_{L,Sp} = \frac{nFDC_0}{r} \tag{10}$$

and for steady-state linear diffusion, j_L, by:

$$j_L = \frac{nFDC_0}{\delta}, \tag{11}$$

where n is the number of transferred electrons, F the Faraday constant, D and C_0 the diffusion coefficient and bulk concentration of the depositing ion, respectively, r the radius of the spherical microelectrode, and δ is the diffusion layer thickness of the macroelectrode. It follows from (10) and (11) that:

$$\frac{j_{L,Sp}}{j_L} = \frac{\delta}{r}. \tag{12}$$

An electrode around which the hydrodynamic diffusion layer can be established, being considerably lower than dimensions of it, could be considered as a macroelectrode. An electrode, mainly spherical, whose diffusion layer is equal to the radius of it, satisfying

$$\delta \gg r \tag{13}$$

can be considered as a microelectrode.[11]

According to (7) for

$$f_c \gg f_a \text{ and } \frac{j_0 f_c}{j_L} \gg 1, \tag{14}$$

the cathodic process on the macroelectrode enters full diffusion control, i.e.,

$$j \cong j_L. \tag{15}$$

Simultaneously, the cathodic current density on the hemispherical microelectrode, j_{Sp}, is given by:

$$j_{Sp} = \frac{j_0(f_c - f_a)}{1 + \dfrac{j_0 f_c}{j_{L,Sp}}} \tag{16}$$

or, because of (12)

$$j_{Sp} = \frac{j_0(f_c - f_a)}{1 + \left(\dfrac{j_0}{j_L}\right)\left(\dfrac{r}{\delta}\right) f_c} \tag{17}$$

and, if condition (14) is also valid, but

$$\frac{r}{\delta} \to 0. \tag{18}$$

Equation (17) can be rewritten in the form

$$j = j_0 f_c. \tag{19}$$

This means that the process on the microelectrode in the bulk solution can be under complete activation control at the same overpotential at which the same process on the macroelectrode is simultaneously under full diffusion control.

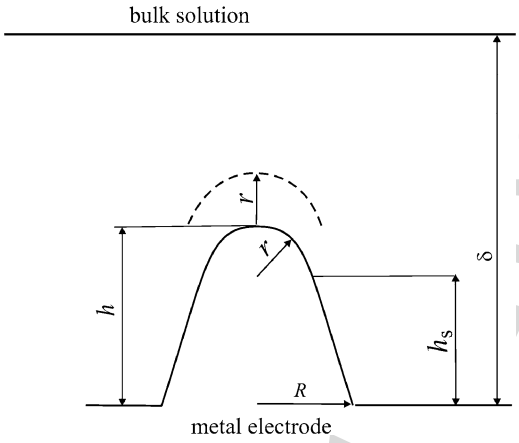

Figure 1. Model of a paraboloidal surface protrusion; h is the height of the protrusion relative to the flat portion of the surface, h_s is the corresponding local side elongation, r is the radius of the protrusion tip, R is the radius of the protrusion base, δ is the thickness of the diffusion layer and $\delta \gg h$. Reprinted from ref. [7] with permission of Elsevier.

Naturally, the microelectrodes can be placed on the macroelectrodes inside their diffusion layers. Let us consider the model of surface irregularities shown in Fig. 1. The electrode surface irregularities are buried deep in the diffusion layer, which is characterized by a steady linear diffusion to the flat portion of the surface.[7,20]

At the side of an irregularity, the limiting diffusion current density, $j_{L,S}$, is given as:

$$j_{L,S} = \frac{nFDC_0}{\delta - h_s} = j_L \frac{\delta}{\delta - h_s}. \quad (20)$$

Obviously, this is valid if the protrusion height does not affect the outer limit of the diffusion layer, and that a possible lateral diffusion flux supplying the reacting ions can be neglected. At the tip of an irregularity, the lateral flux cannot be neglected and the situation can be approximated by assuming a spherical diffusion current density, $j_{L,tip}$, given by:[20]

$$j_{L,tip} = \frac{nFDC^*}{r} \quad (21)$$

where C^* is the concentration of the diffusing species at a distance r from the tip, assuming that around the tip a spherical diffusion layer having a thickness equal to the radius of the protrusion tip is formed. If deposition to the macroelectrode is under full diffusion control, the distribution of the concentration C inside the linear diffusion layer is given by:[12]

$$C = C_0 \frac{h}{\delta}, \tag{22}$$

where $0 \leq h \leq \delta$. Hence,

$$C^* = C_0 \frac{h + r}{\delta} \tag{23}$$

and

$$j_{L,tip} = j_L \left(1 + \frac{h}{r}\right) \tag{24}$$

because of (11), (21), and (23).

The tip radius of the paraboloidal protrusion is given by[11–13]

$$r = \frac{R^2}{2h} \tag{25}$$

and substitution of r from (25) in (24) gives

AQ2

(26)

or

$$j_{L,tip} = j_L(1 + 2k^2), \tag{27}$$

where

$$k = \frac{h}{R}. \tag{28}$$

If $h = R$, $k = 1$, hence for a hemispherical protrusion,

$$j_{L,tip} = 3 j_L \tag{29}$$

If $h \ll R$, $k \to 0$,

$$j_{L,tip} \to j_L \tag{30}$$

and if $R \ll h$, $k \to \infty$ and

$$j_{L,tip} \to \infty. \tag{31}$$

Substitution of $j_{L,tip}$ from (27) instead of j_L in (7) and further rearranging give:

$$j_{tip} = \frac{j_0(f_c - f_a)}{1 + \left(\frac{j_0}{j_L} \cdot \frac{1}{1 + 2k^2} f_c\right)}. \tag{32}$$

The current density on the tip of a protrusion, j_{tip}, is determined by k, hence by the shape of the protrusion. If $k \to 0$, $j_{tip} \to j$ (see (7)) and if $k \to \infty$, $j_{tip} \to j_0(f_c - f_a) \gg j$. The electrochemical process on the tip of a sharp needle-like protrusion can be under pure activation control outside the diffusion layer of the macroelectrode. Inside it, the process on the tip of a protrusion is under mixed control, regardless it is under complete diffusion control on the flat part of the electrode for $k \to 0$. If $k = 1$, hence for hemispherical protrusion, j_{tip} will be somewhat larger than j, but the kind of control will not be changed. It is important to note that the current density to the tip of hemispherical protrusion does not depend on the size of it if $k = 1$. This makes a substantional difference between spherical microelectrodes in bulk solution and microelectrodes inside diffusion layer of the macroelectrode.[16] In the first case, the limiting diffusion current density depends strongly on the radius of the microelectrode.

Taking into account that the exchange current density depends on the concentration of reacting ion, it follows that the growth of dendrites[12,21,22] inside the diffusion layer of the macroelectrode is in fact under mixed activation–diffusion control. Hence, it can be expected that the process on the microelectrodes placed on the surface of the inert macroelectrode can be under mixed control. This is because the charge transfer occurs on the microelectrodes, while the mass-transfer limitations are related to the diffusion layer of the macroelectrode.

III. INERT MACROELECTRODE PARTIALLY COVERED WITH HEMISPHERICAL ACTIVE MICROELECTRODES

1. Mathematical Model

The use of microelectrodes is impractical, but the use of ensembles of microelectrodes can be a real option. The ensemble of microelectrodes consists of microelectrodes placed on the inert surface at distances between their centers larger than their diameter.

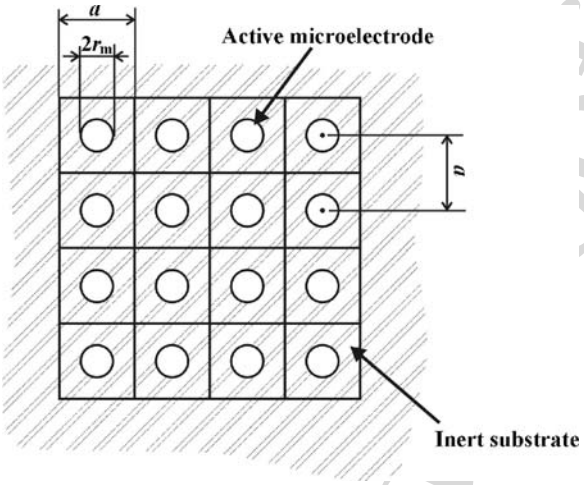

Figure 2. A schematic presentation of the top view of the surface of an inert macroelectrode modified with microelectrodes of catalyst. Reprinted from ref. [7] with permission of Elsevier.

Assuming homogeneously distributed, equal to each other, hemispherical grains of the catalyst on an inert substrate, in a way similar to that used by Gileadi[16] to describe an ensemble of microelectrodes, the surface of the macroelectrode can be presented by an idealized model, as in Fig. 2, and the number of grains per square centimeter is given by:

$$N = \frac{1}{a^2}. \tag{33}$$

It is obvious from Fig. 2 that the edge size, a, of a square of the surface of the inert macroelectrode belonging to one such particle is equal to the distance between the centers of the closest particles. If

$$a = x \cdot 2r_{\mathrm{m}}, \tag{34}$$

where r_{m} is the radius of the microelectrode and x is the ratio of the distance between the centers of the particles and the particle diameter, and (33) can be rewritten in the form

$$N = \frac{1}{4r_{\mathrm{m}}^2 \cdot x^2}. \tag{35}$$

The surface of each hemispherical microelectrode, S_m, is

$$S_m = 2r_m^2 \cdot \pi \,, \tag{36}$$

and the working surface of catalyst per square centimeter of macroelectrode, S_w, is then

$$S_w = N \cdot S_m = \frac{\pi}{2x^2} \tag{37}$$

or

$$S_w = \frac{2r_m^2 \pi}{a^2} \tag{38}$$

if (34) is taken into account, being dependent on the ratio r_m/a.

A schematic presentation of the cross section of the diffusion layer of an inert macroelectrode partially covered with small active hemispherical particles is shown in Fig. 3, taking into account that $\delta \gg r_m$.

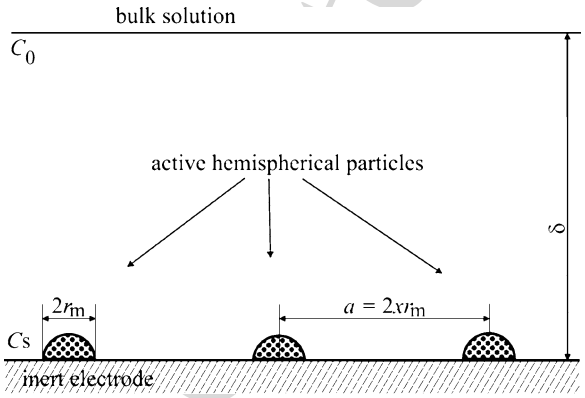

Figure 3. Schematic presentation of the cross section of the diffusion layer of a partially covered inert electrode with hemispherical active particles, where r_m is the radius of the microelectrodes, δ is the diffusion layer thickness of the macroelectrode, C_0 and C_S are the bulk and the surface concentrations of reacting ions, respectively, x is the ratio of the distance between the centers of neighboring particles and the particle diameter, and $\delta \gg r$. Reprinted from ref.[7] with permission of Elsevier.

A mathematical model can be derived under the assumption that the electrochemical process on the microelectrodes inside the diffusion layer of a partially covered inert macroelectrode is under activation control, despite the overall rate being controlled by the diffusion layer of the macroelectrode. The process on the microelectrodes decreases the concentration of the electrochemically active ions on the surfaces of the microelectrodes inside the diffusion layer of the macroelectrode, and the zones of decreased concentration around them overlap, giving way to linear mass transfer to an effectively planar surface.[15] Assuming that the surface concentration is the same on the total area of the electrode surface, under steady-state conditions, the current density on the whole electrode surface, j, is given by:

$$j = \frac{nFD(C_0 - C_S)}{\delta}, \tag{39}$$

where n is the number of transferred electrons, F the Faraday constant, and D is the diffusion coefficient of the reacting ion. Obviously, the current density from (39) is due to the difference in the bulk, C_0, and surface concentration, C_S, of the reactive ion. The concentration dependence of the exchange current density[22] is expressed as

$$j_{0,S} = \left(\frac{C_S}{C_0}\right)^{\gamma} j_0, \tag{40}$$

where

$$\gamma = \frac{d \log j_0}{d \log C_0} \tag{41}$$

and j_0 is the exchange current density for a surface concentration C_0 equal to that in the bulk, and $j_{0,S}$ is the exchange current density for a surface concentration C_S.

The current density on the macroelectrode can also be written as:

$$j = S_w j_0 \left(\frac{C_S}{C_0}\right)^{\gamma} (f_c - f_a) \tag{42}$$

assuming a reversible activation controlled electrode process on the hemispherical active microelectrodes on an inert substrate, where S_w is the active surface per square centimeter of the macroelectrode and j_0 is the exchange current density on the massive active electrode, standardized to the apparent electrode surface.

The current densities given by (39) and (42) are mutually equal and substitution of C_S/C_0 from (39) into (42), taking also into account (11) gives:

$$j = S_w j_0 \left(1 - \frac{j}{j_L}\right)^{\gamma} (f_c - f_a) \tag{43}$$

or, for $\gamma = 1$, after rearranging

$$j = \frac{S_w j_0 (f_c - f_a)}{1 + \dfrac{S_w j_0 (f_c - f_a)}{j_L}}, \tag{44}$$

where j_L is the limiting diffusion current density on the macroelectrode, standardized to the apparent electrode surface.

It is necessary to note that (44) is an approximation, because the value of γ is lower than unity. This approximation is widely used in qualitative discussions, because it permits the simple mathematical treatment of electrochemical processes with relatively small errors and with clear physical meaning. If $\gamma \neq 1$ is included in the derivation of the general polarization curve equation, simple analytical solutions are not available and numerical solutions are required.

It is obvious that

$$j_{0,\mathrm{eff}} = S_w j_0 \tag{45}$$

is the effective value of the exchange current density relative to the total surface of a partially covered electrode. It was shown[23] that the activity of a gold electrode modified with platinum 3D islands with 72% active Pt sites on the electrode is approximately 25% smaller than with pure platinum. This result is in excellent agreement with (45).

As stated earlier, (44) with $\gamma = 1$ is more suitable for discussion, but the calculation will be performed using (43) and the value of $\gamma = 0.5$ for the one-electron transfer process.[7]

Equation (44) is the polarization curve equation for a modified inert electrode for $\gamma = 1$. It is valid for inert substrates modified by active microparticles or nanoparticles as well as by 2D and 3D islands of active metal.

If

$$f_c \gg f_a \text{ and } \frac{S_w j_0 f_c}{j_L} \ll 1. \tag{46}$$

Equation (44) becomes:

$$j = S_w j_0 f_c \tag{47}$$

and for

$$f_c \gg f_a \text{ and } \frac{S_w j_0 f_c}{j_L} \gg 1. \tag{48}$$

Equation (44) becomes:

$$j \cong j_L \tag{15}$$

meaning that j_L does not depend on S_w.

If

$$f_c > f_a \text{ and } \frac{S_w j_0 (f_c - f_a)}{j_L} \gg 1. \tag{49}$$

Equation (15) is also valid, meaning that the process is under complete diffusion control at all overpotentials when $j_0 \to \infty$ if $j_L > 0$ and $S_w > 0$.

An important conclusion can be drawn from the above derivations. If (46) and (47) are valid, only a part of the surface covered with catalyst is active, with an exchange current density corresponding to the massive catalyst which makes all the electrode surface active but with a proportionally lower exchange current density.

If (48) and (15) are valid, the process enters complete diffusion control, and overpotential required increases with a decrease of S_w.

If (49) and (15) are valid, even for small S_w and overpotentials, all the surface behaves as an active one if $j_0/j_L \to \infty$. This means that the application of a partially covered inert substrate with active micro and nanoparticles will be more effective for the cases of fast electrochemical reactions. It is obvious that the above reasoning is valid not only for an inert substrate covered with microparticles, but also for any kind of partially covered electrode.

2. Polarization Curves

(i) Calculated Ohmic Potential Drop Is Not Included

The real situation can be estimated by digital simulation.[7,24] It will be performed for example for one-electron transfer process and $\beta = 0.5$ and $\gamma = 0.5$.[7] In all cases, the apparent current density is standardized to the apparent surface of modified electrode.

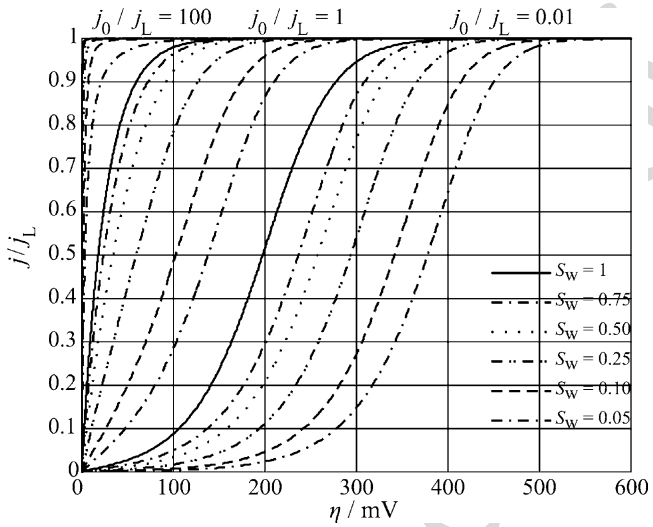

Figure 4. Dependences $j/j_L - \eta$ calculated from (43), using $j_0/j_L = 100$, 1 and 0.01, $S_w = 0.05$, 0.1, 0.25, 0.5, 0.75 and 1, and $f_c = 10^{\frac{\eta}{120}}$, $f_a = 10^{-\frac{\eta}{120}}$, and $\gamma = 0.5$ (Reprinted from ref.[7] with permission from Elsevier).

Using (43) with $\gamma = 0.5$ and $j_0/j_L = 100$, 1, and 0.01, $S_w = 0.05$, 0.1, 0.25, 0.5, 0.75, and 1, and $f_c = 10^{\eta/120}$ and $f_a = 10^{-\eta/120}$, the diagrams presented in Fig. 4 are obtained. The current density–overpotential dependence above each set of polarization curves corresponds to $S_w = 1$. It follows from Fig. 4. that for large values of $j_{0,eff}/j_L$, electrochemical polarization can probably be neglected and that complete Ohmic control of the deposition process can be expected, for $j_{0,eff}/j_L \geq 100$ up to a current density about $0.95\,j_L$ and for $j_{0,eff}/j_L = 0.5$ for current densities lower than $0.3\,j_L$.

As told earlier, the shape of polarization curves does not depend strongly on S_w at large j_0/j_L ratios. At lower ones, the important effect arises.

In Fig. 5, polarization curves for $j_0/j_L = 100$, 1, and 0.01 and $S_w = 1$ (other parameters as in the caption of Fig. 4) were calculated using (43) and (44).

It can be seen from Fig. 5 that the approximation of (43) by (44) is acceptable at all overpotentials and ratios j_0/j_L, being completely

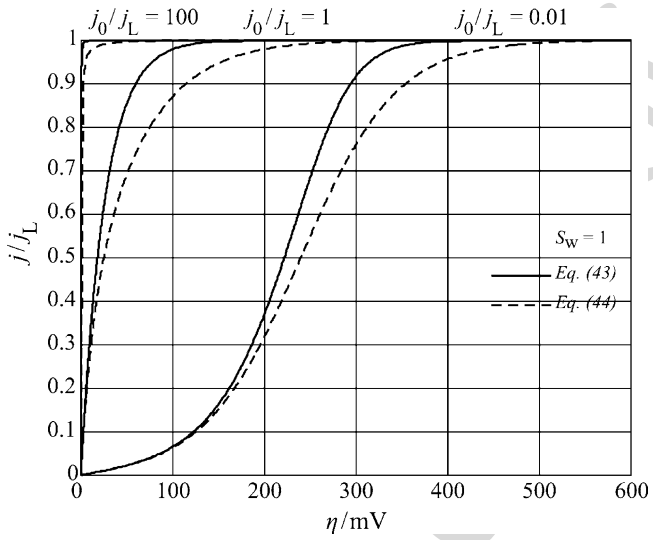

Figure 5. The same as in Fig. 4 but for $j_0/j_L = 100$, 1 and 0.01, $S_w = 1$, using (43) and $\gamma = 0.5$ as well as (44). Reprinted from ref. [7] with permission from Elsevier.

correct at low overpotentials for low exchange current densities (the Tafel region) and at large values of j_0/j_L at all overpotentials.

Finally, (7) and (44) should be compared with each other. Taking $j_0/j_L = 100$, 10, 1, 0.1, and 0.01, $S_w = 1$, and $f_c = 10^{\eta/120}$ and $f_a = 10^{-\eta/120}$, the diagrams presented in Fig. 6 are obtained. It can be seen that for $j_0/j_L \leq 1$ diagrams computed using (7) and (44) are the same. This can be explained in the following way.

Equation (7) is valid for the complete active electrode surface. On the other hand, if the inert substrate is partially covered with the same active material, the polarization curve equation is given by (44).[7]

Using the recently derived equation (44), it was possible to elucidate the Ohmic-controlled electrodeposition of metals by the consideration of silver electrodeposition on the graphite electrode, where each microelectrode was independent relative to the other ones.

At larger values of j_0/j_L ratio, the polarization curves calculated by (7) exhibit complete diffusion control being practically the same as follows from (7) when $j_0/j_L \to \infty$, for $f_c > f_a$. On the other

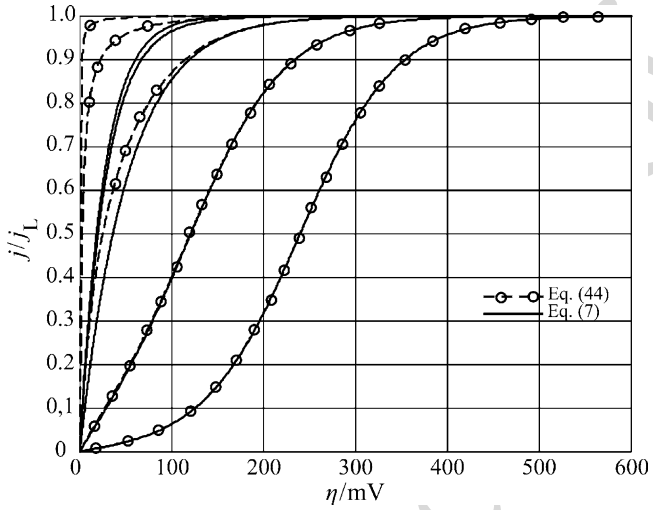

Figure 6. The comparison of polarization curves calculated using (7) and (44). From left to right side of diagram j_0/j_L ratio corresponds to 100, 10, 1, 0.1 and 0.01, respectively; $f_c = 10^{\frac{\eta}{120}}$, $f_a = 10^{-\frac{\eta}{120}}$, and $S_w = 1$. Reprinted from ref. [8] with permission of Elsevier.

hand, polarization curves calculated using (44) under the same conditions become

$$j \cong j_L. \tag{15}$$

The current densities on the massive electrode of the active material and on the inert electrode activated with microelectrodes of the same material become equal at

$$S_w = \frac{1}{1 + \frac{j_0}{j_L} f_a} \tag{50}$$

as follows from (7) and (44), being strongly dependent on the j_0/j_L ratio.[8] Obviously, for electrochemical processes characterized with $j_0/j_L \gg 1$, the inert electrode will behave as a massive active one even at low coverage. On the other hand, if $j_0/j_L \ll 1$, it follows from (50) that inert electrode will behave as activated one at $S_w = 1$.

Naturally, during deposition on the same substrate, it can be expected that only small part of the electrode surface will be active

and that for $j_0/j_L \rightarrow \infty$ (44) is valid on both the inert and the same active substrate. It can be seen from Fig. 6 that the increase of the value of j_0/j_L ratio leads to the decrease of the electrochemical overpotential. The activation part of overpotential is lost at j_0/j_L values larger than 10, while both activation and diffusion overpotential vanish at j_0/j_L values larger than 100 (Fig. 6). In the second case, the Ohmic-controlled electrochemical reaction can occur.

The Ohmic potential drop is not included in the polarization curves depicted in Figs. 4–6.

The increase of the value of the j_0/j_L ratio produces large saving of energy.

(ii) Calculated Ohmic Potential Drop Included

The polarization curves for the electrodeposition process, which include the Ohmic voltage drop, can be obtained as follows, assuming $S_w = 1$ in all cases.[7,9,24] This will be performed for a one-electron transfer process and $\beta = 0.5$, meaning $\gamma = 0.5$.[7]

Using (43) with $\gamma = 0.5$ and $j_0/j_L = 100$, 10, 1, and 0.01, $f_c = 10^{\eta/120}$ and $f_a = 10^{-\eta/120}$, and $j_L = 50$ and 10 mA cm^{-2}, the dependences presented by the dashed line in Figs. 7–10 are obtained. The Ohmic potential drop is not included in the calculated polarization curves depicted in Figs. 7–10 by the dashed line. It follows from Figs. 7–10 that for large values of j_0/j_L, electrochemical polarization can probably be neglected but mass-transfer limitations are present in all cases, which can also be shown by differentiation of (7).

On the other hand, the measured value of overpotential, η_m, is given by:

$$\eta_m = \eta + j\frac{L}{\kappa} \tag{51}$$

due to the *IR* error,[25] where L is the length of the electrolyte column between the tip of a liquid capillary and the electrode and κ is the specific conductivity of the electrolyte.

For a 1 M solution of a typical fully dissociated electrolyte, the value of κ is around 0.1 S cm^{-1}, L can be taken as 0.2 cm, and $j_L =$ 50 mA cm^{-2} and 10 mA cm^{-2}. Using these given values, as well as $\kappa = 0.033$ S cm^{-1}, (51), and the diagrams presented in Figs. 7–10 by the dashed line, polarization curves including the Ohmic potential drop can be obtained, as shown in Figs. 7–10 by the solid line.

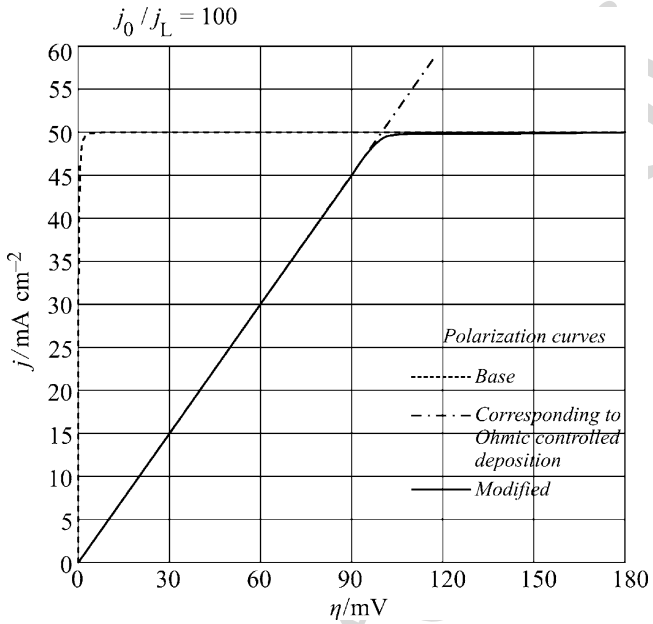

Figure 7. The dependence $j - \eta$ calculated using (43), $j_0/j_L = 100$, $f_c = 10^{\frac{\eta}{120}}$, $f_a = 10^{-\frac{\eta}{120}}$, $\gamma = 0.5$, $S_w = 1$ and $j_L = 50\,\mathrm{mA\,cm^{-2}}$, and one modified using (51), $L = 0.2\,\mathrm{cm}$, $\kappa = 0.1\,\mathrm{s\,cm^{-1}}$. Reprinted from ref. [9] with permission from Elsevier.

Naturally, the condition of Ohmic-controlled electrochemical process can be derived from (51) as:

$$\eta \ll j\frac{L}{\kappa} \tag{52}$$

or

$$\eta \leq 0.01\, j\frac{L}{\kappa}. \tag{53}$$

In the case under consideration, complete Ohmic control of the deposition process can be expected for $j_0/j_L \geq 100$ up to a current density about $0.95\,j_L$ (Fig. 7) and for $j_0/j_L = 10$ up to $0.6\,j_L$ (Fig. 9). It is obvious from Figs. 7–10 that, regardless of the shape of the polarization curve, which depends on the j_0/j_L ratio and κ, a limiting diffusion current density plateau is present in all cases.

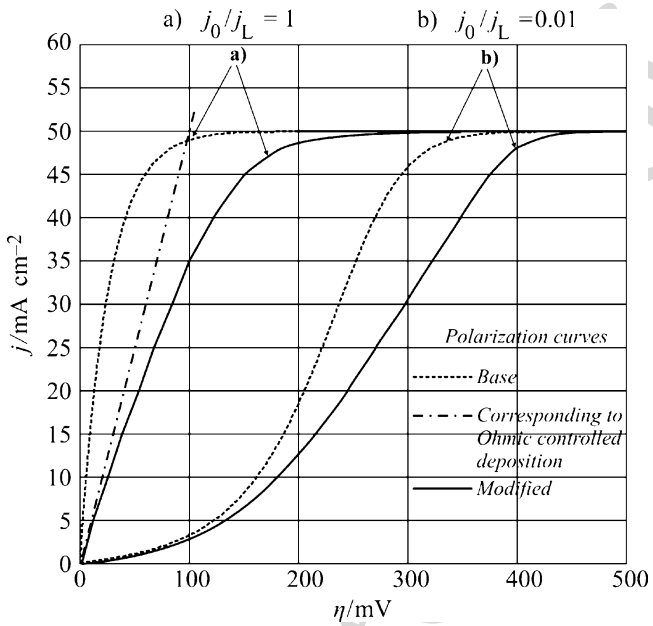

Figure 8. The dependences $j - \eta$ calculated using (43), $j_0/j_L = 1$ and 0.01, $f_c = 10^{\frac{\eta}{120}}$, $f_a = 10^{-\frac{\eta}{120}}$, $\gamma = 0.5$, $S_w = 1$ and $j_L = 50\,\text{mA cm}^{-2}$, and ones modified using (51), $L = 0.2$ cm, $\kappa = 0.1\,\text{s cm}^{-1}$. Reprinted from ref. [9] with permission from Elsevier.

Obviously, increasing the concentration of the reacting ion and decreasing the concentration of the supporting electrolyte in a simple salt solution stimulates Ohmic control of the deposition process, but a large value of the exchange current density seems to be the most important for it (Figs. 9 and 10).

It can be noted that before the increase of the current density, over the value of the limiting diffusion one, the first part of the polarization curve for silver deposition from nitrate solution[7] has practically the same shape as that from Fig. 7 and that those from Fig. 8 are very similar to the ones for Cd and Cu deposition.[26] The value of j_0 for Ag deposition is very large.[27] In the cases of both Cd[28] and Cu[29] deposition, j_0 is considerably lower than in the case of Ag deposition.

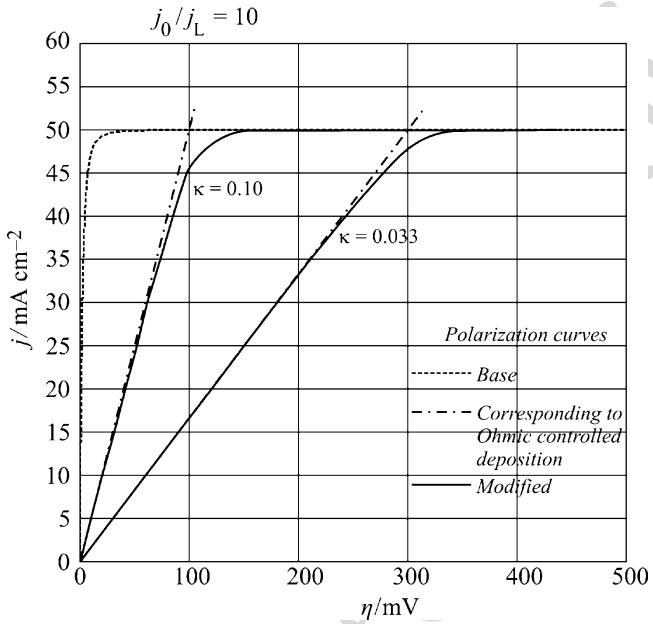

Figure 9. The dependences $j - \eta$ calculated using (43), $j_0/j_L = 10$, $f_c = 10^{\frac{\eta}{120}}$, $f_a = 10^{-\frac{\eta}{120}}$, $\gamma = 0.5$, $S_w = 1$ and $j_L = 50\,\mathrm{mA\,cm^{-2}}$, and ones modified using (51), $L = 0.2\,\mathrm{cm}$, $\kappa = 0.1$ and $0.033\,\mathrm{S\,cm^{-1}}$. Reprinted from ref. [9] with permission from Elsevier.

The increase in the current density over the limiting diffusion current in the absence of some other electrochemical process indicates a decrease of the mass transport limitations, due to initiation of growth of dendrites and further dendritic growth.

3. Experimental Verification

The polarization characteristic of a partially covered inert macroelectrode is easy to determine, but it is very difficult or even impossible to do the same for microelectrodes placed on it. On the other hand,[30] the morphology of metal electrodeposits indicates the conditions of deposition. Hence, the type of process control on the microelectrodes can be derived from their morphology and correlated with the polarization curve for the partially covered macroelectrode.

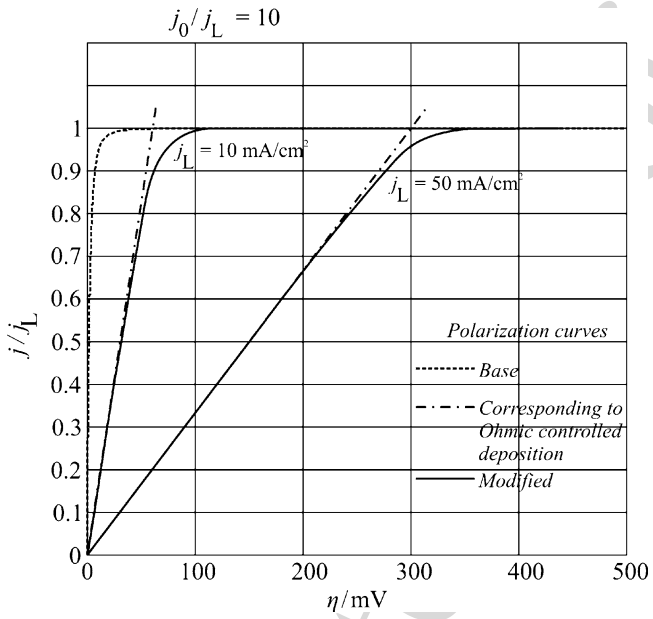

Figure 10. The dependences $j/j_L - \eta$ calculated using (43), $j_0/j_L = 10$, $f_c = 10^{\frac{\eta}{120}}$, $f_a = 10^{-\frac{\eta}{120}}$, $\gamma = 0.5$, $S_w = 1$, $j_L = 10\,\mathrm{mA\,cm^{-2}}$ and $j_L = 50\,\mathrm{mA\,cm^{-2}}$, and ones modified using (51), $L = 0.2\,\mathrm{cm}$, $\kappa = 0.033\,\mathrm{S\,cm^{-1}}$. Reprinted from ref. [9] with permission from Elsevier.

There are two conditions under which the particles of active metal placed on the surface of a macroelectrode can represent microelectrodes. The first condition is that the substrate is conducting but inert relative to the process under consideration. The second one is that the grains are sufficiently small to permit activation control of the electrochemical process on them, making thus, mixed overall control, as in the case of the tips of growing dendrites,[11,12,31] or during the induction time of the formation of spongy deposits.[32–34]

As already stated, the nuclei behave as microelectrodes in the initial stage of electrodeposition of metals onto inert substrates.[33] If nucleation exclusion zones around nuclei are formed,[35,36] an inert substrate can be partially covered even at long deposition times, due to the nucleation exclusion zones overlapping, which results in the formation of granular electrodeposits.[37,38] In this way, a granular

silver deposit on a platinum or graphite electrode can represent the ideal physical model of an inert substrate covered by nanoparticles.

It was shown earlier[32,33] that the mechanism of spongy deposit formation can be successfully illustrated by a physical model and that the calculations derived for the real system can be applied for the model and vice versa. The formation of nucleation exclusion zones is illustrated by the physical model[35] as well as by the effect of the exchange current density of the deposition process on the radii of them[36,39] with fair agreement with the experimental data. In addition, the physical simulation[40,41] of the periodicity in the surface structure of a polycrystalline electrolytic deposit[42] is also possible. As nucleation rings appear due to the supersaturation zones,[40] the mutual effect of the nuclei at the moment of their formation confirms directly that the process on the nanoscale can also be elucidated by an appropriate physical model. Besides, even the electrochemical treatment of tumors in human tissue can be simulated by the electrochemical model.[43] Hence, it can be expected that physical modeling will also be useful in the consideration of mass transfer on an inert electrode partially covered with small particles of an active metal. The kind of a process control on the microelectrodes inside the diffusion layer of a partially covered inert electrode could be estimated, and a mathematical model of the overall process on a partially covered electrode proposed.

The electrolyte solutions used in further experiments were: 0.5 M $AgNO_3$ in 0.2 M HNO_3 (nitrate bath) and 0.1 M $AgNO_3$ in 0.5 M $(NH_4)_2SO_4$ (ammonium bath). The overpotential was increased from initial to the final value and held for 30 s before measurement in all cases during the polarization measurements.

The polarization curves for silver electrodeposition are presented in Fig. 11.

It is obvious from Fig. 11 that the polarization curves for deposition on the compact silver layer and on the uncovered graphite electrode are practically the same. In both cases, the Ohmic-controlled deposition is obvious. This can mean that the deposition on the graphite electrode coated with silver also initiates by nucleation. Besides, the grain of silver can be seen from Fig. 12a. In both cases, an overpotential of 120 mV belongs to the region in which a slight decline in the slope of the polarization curve indicates an increased degree of diffusion control. At overpotentials larger than 140 mV, a strong increase in the current density with increasing overpotential occurs because of the initiation of dendritic growth.[11,12]

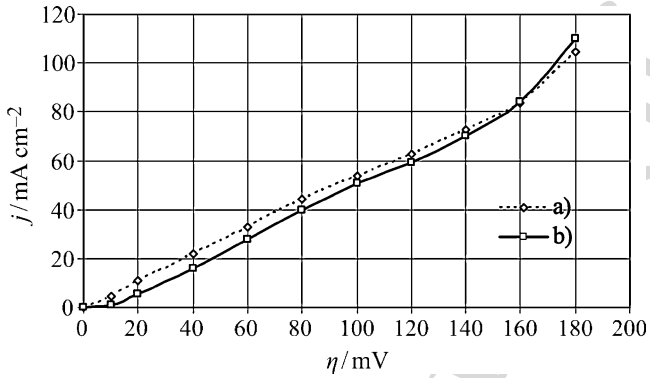

Figure 11. Polarization curves for silver electrodeposition from the nitrate solution on: (**a**) a graphite electrode previously plated with silver from the ammonium solution; (**b**) on an uncovered graphite electrode. Reprinted from ref. [7] with permission from Elsevier.

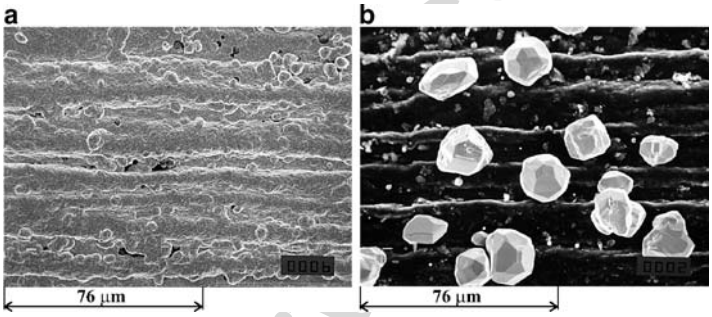

Figure 12. The physical model of a partially covered inert electrode with active grains and a completely covered inert electrode: (**a**) a graphite electrode completely covered by deposition from the ammonium bath; current density on the electrode completely covered with silver was 62.5 mA cm^{-2} at an overpotential of 120 mV in the nitrate solution; magnification 500×; (**b**) the silver deposit on the graphite electrode after the polarization measurements ended at an overpotential of 120 mV in the nitrate solution; magnification 500×; current density on such electrode was 59.4 mA cm^{-2} at the same overpotential in the nitrate solution. Reprinted from ref. [7] with permission of Elsevier.

The polarization curves on platinum electrodes were very similar to those obtained on graphite ones.[7]

An SEM microphotograph of the silver deposit obtained after polarization measurement up to an overpotential of 120 mV on an

uncovered graphite electrode is shown in Fig. 12b. The electrode surface is partially covered because of the overlapping of the nucleation exclusion zones, being, as already told, the ideal physical model of a partially covered inert electrode.

The surface of completely covered graphite electrode by deposition from ammonium bath is shown in Fig. 12a. The regular crystal form of the grains in Fig. 12b confirms that the deposition on the microelectrodes is not under diffusion control,[44,45] despite the overall deposition rate being determined by diffusion to the macroelectrode.

The current density on the electrode from Fig. 12b, with a coverage of about 20%, is practically the same as on a completely covered graphite electrode, as can be seen from Fig. 11 at an overpotential of 120 mV. This is because the exchange current density for the silver electrodeposition process from nitrate baths is extremely large.[27,46]

A similar situation appears in silver electrodeposition on platinum.[7]

The surface layers of silver obtained by electrodeposition from an ammonium bath on a graphite electrode are shown in Fig. 13.

The S_w in Fig. 13a is about 20% and the current density at 30 mV is about 40% of the current density on a completely covered

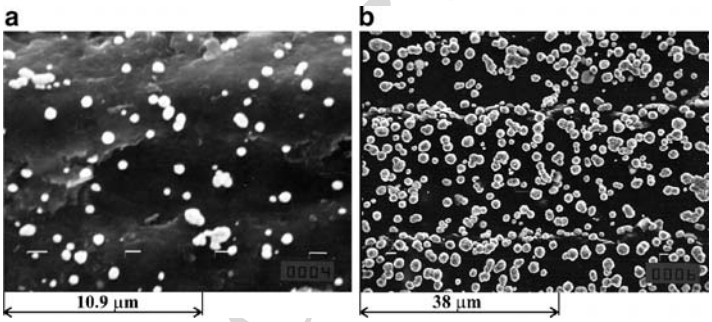

Figure 13. The silver layer on a graphite electrode obtained by electrodeposition from the ammonium solution at an overpotential of 100 mV for: (**a**) 2.5 s. The current density on this electrode in the ammonium solution at an overpotential of 30 mV was 0.5 mA cm^{-2}. Magnification 3,500×; (**b**) 60 s. The current density on this electrode in the ammonium solution at an overpotential of 30 mV was 1.0 mA cm^{-2}. The current density on a completely covered graphite electrode after a pulse of an overpotential of 150 mV for 3 s and deposition at an overpotential of 100 mV for 10 min was 1.25 mA cm^{-2} at the same potential. Magnification 1,000×. Reprinted from ref. [7] with permission from Elsevier.

inert substrate in ammonium solution. In Fig. 13b, the S_w is more than 90% and current density is 80% of the current density on a completely covered electrode. This is in accordance with (44) and (47), because the exchange current density for the silver electrodeposition process from ammonium solutions is considerably lower than the corresponding limiting diffusion current density.[47]

The above facts are a fair illustration of the concluding remarks in the previous section. It is necessary to note that the uncovered part of the inert substrate after nucleation at larger potentials negative to the reference electrode remains inert at lower ones.

4. The Required Quantity of Active Substance

Finally, the required quantity of catalyst for the activation of an inert substrate can now be estimated as follows. The volume of hemispherical microelectrode, V_m, is given by

$$V_m = \frac{2}{3} r_m^3 \cdot \pi \tag{54}$$

and the mass of such a grain is then

AQ4 (55)

where ρ is the density of catalyst, and the mass of catalyst per square centimeter of the inert electrode, m, is

$$m = N \cdot m_m = \frac{r_m \cdot \pi \cdot \rho}{6x^2} \tag{56}$$

or, taking into account (37) and (50)

$$m = \frac{r_m \cdot \rho}{3} S_w = \frac{r_m \cdot \rho}{3} \cdot \frac{1}{1 + \frac{j_0}{j_L} f_a}. \tag{57}$$

Equation (57) is valid for the cathodic processes. In similar way, the corresponding equation for the anodic ones can be derived.

It is obvious from (57) that the quantity of catalyst in the form of small hemispherical grain required to transform an inert electrode into an active one decreases rapidly with decrease in size of the particles, for one and the same S_w, as well as with the increase of the

j_0/j_L value for the process taking place on it. Hence, (57) can be considered as fundamental one for electrocatalysis by active particles on inert electrodes.

The current density on the graphite electrode partially covered with silver grains obtained from the nitrate solution by a pulse of an overpotential of 100 mV for 20 ms and by further growth at an overpotential of 40 mV for 30 s (Fig. 14a) is practically the same as the current density on a massive silver electrode at an overpotential of 40 mV. The same occurs with a graphite electrode covered with silver grains by a pulse of an overpotential of 500 mV for 5 ms and by further growth at an overpotential of 40 mV for 5 s (Fig. 14b). It can be seen that the deposits depicted in Fig. 14a and this in Fig. 14b,

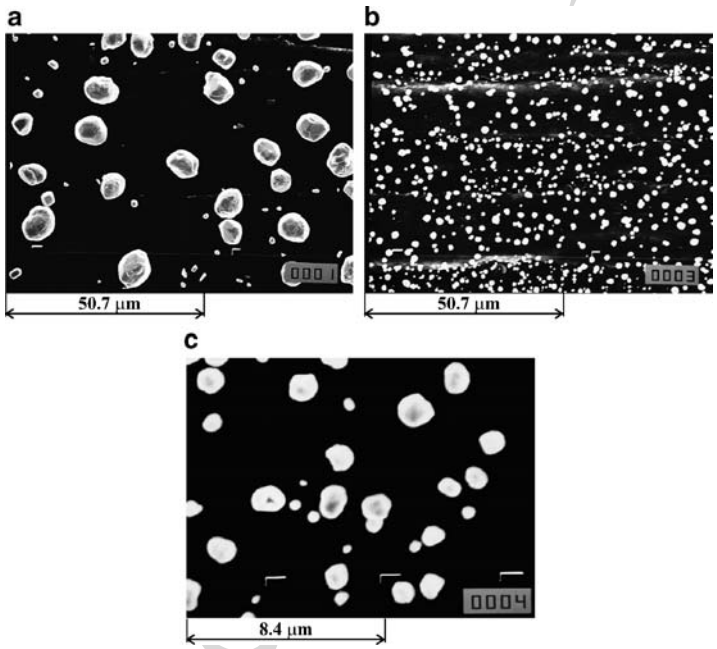

Figure 14. Silver electrodeposits on a graphite electrode obtained from the nitrate solution: (**a**) pulse of an overpotential of 100 mV for 20 ms and further growth at an overpotential of 40 mV for 30 s. Magnification 750×; (**b**) pulse of an overpotential of 500 mV for 5 ms and further growth at an overpotential of 40 mV for 5 s; magnification 750×; (**c**) the same as in (**b**), but under a magnification of 4,500×. Reprinted from ref. [7] with permission of Elsevier.

under the same magnification, are very different. In Fig. 14c, the deposit from Fig. 14b, but under a considerably larger magnification, is shown, being very similar to that depicted in Fig. 14a.

It seems to be practically identical with the deposit shown in Fig. 14a, which can also be concluded from calculated $x/2r_m$ values, being 2.5 for the deposit shown in Fig. 14a and 2.9 for that shown in Fig. 14b. It is obvious that despite the grains being many times smaller, their mutual relations are similar to those shown in Fig. 14a, producing the same activity with a many times lower quantity of electrodeposited metal, which is in the accordance with (37) and (38).

In both cases, the current density on the partially covered electrode was 21 mA cm^{-2}. The current density on a completely covered graphite electrode in the nitrate solution was 22 mA cm^{-2} at an overpotential of 40 mV.

The electrodeposition of metals on inert substrates by fast electrochemical reactions permits the physical modeling of processes on partially covered inert substrates due to formation of nucleation exclusion zones around the growing grains. Regardless of the continuous change of the size of the microelectrodes during the deposition process, the current density and morphology can be correlated to each other after any deposition time. It is also the only way of determining the type of process control on the microelectrodes.

Hence, the procedure described above could be unavoidable for the elucidation of the polarization behavior of an inert electrode partially covered with small active grains, probably with nanoparticles, too.

IV. INERT ELECTRODES ACTIVATED WITH DENDRITES

1. Large Level of Coarseness

From the electrochemical point of view, a dendrite can be defined as an electrode surface protrusion that grows under activation or mixed control, while deposition to the flat part of the electrode surface is under complete diffusion control.[11–13,48]

Considering the model of surface irregularities shown in Fig. 1, the surface irregularities are buried deep in the diffusion layer, which is characterized by a steady linear diffusion to the flat portion of completely active surface.

If the protrusion does not affect the outer limit of the diffusion layer, i.e., if $\delta \gg h$, the limiting diffusion current density to the tip of the protrusion from Fig. 1, $j_{L,tip}$, is given by[20]

$$j_{L,tip} = j_L \left(1 + \frac{h}{r}\right). \tag{24}$$

Substitution of $j_{L,tip}$ from (24) into (7) produces for $h/r \gg 1$:

$$j_{tip} = j_{0,tip}(f_c - f_a), \tag{58}$$

where $j_{0,tip}$ is the exchange current density at the tip of a protrusion.

Obviously, deposition to the tip of such protrusion inside the diffusion layer is activation controlled relative to the surrounding electrolyte, but it is under mixed activation–diffusion control relative to the bulk solution.

If deposition to the flat part of electrode is a diffusion-controlled process and assuming a linear concentration distribution inside the diffusion layer, the concentration C at the tip of a protrusion can be given by (22).[12]

$$C = C_0 \frac{h}{\delta}. \tag{22}$$

According to Newman,[22] the exchange current density at the tip of a protrusion is given by

$$j_{0,tip} = j_0 \left(\frac{C}{C_0}\right)^{\gamma} \tag{59}$$

or

$$j_{0,tip} = j_0 \left(\frac{h}{\delta}\right)^{\gamma} \tag{60}$$

because of (22).

Taking into account (58), the current density to the tip of a protrusion is then given by

$$j_{tip} = j_0 \left(\frac{h}{\delta}\right)^{\gamma} (f_c - f_a), \tag{61}$$

being under mixed control due to the $(h/\delta)^{\gamma}$ term, which takes into account the concentration dependence of $j_{0,tip}$, expressing in this way a mixed-controlled electrodeposition process.

Outside the diffusion layer $h \geq \delta$, and (61) becomes:

$$j_{\text{tip}} = j_0(f_c - f_a) \tag{62}$$

indicating pure activation control, as the $(h/\delta)^{\gamma}$ term is absent.

On the other hand, according to Wranglen,[49] a dendrite is a skeleton of a monocrystal and consists of a stalk and branches, thereby resembling a tree.

Dendritic growth occurs selectively at three types of growth sites: at screw dislocations[12] on the indestructible reentrant groove formed in the twinning process[50] and, in the case of a hexagonal close-packed lattice, growth leading to the formation of low index planes.[51] Deposition to the tip of a screw dislocation can be theoretically considered as diffusion to a point and in other two cases as diffusion to a line. In any case, the conditions requested for activation-controlled deposition are fulfilled.[12,52–54]

The current density to the tip of a protrusion formed on the flat part of the electrode surface growing inside the diffusion layer should be larger than the corresponding limiting diffusion current density.[21] Hence, if $\delta \gg h$ and

$$j_L < j_{\text{tip}}, \tag{63}$$

the protrusion grows as a dendrite.

In accordance with (63), instantaneous dendrite growth is possible at overpotentials larger than some critical value, η_{cr}, which can be derived from (61) as shown by Popov et al.[55]

$$\eta_{cr} = \frac{b_c}{2.3} \ln \frac{j_L}{j_0} \left(\frac{\delta}{h}\right)^{\gamma} \tag{64}$$

for $f_c \gg f_a$, where h and δ are the protrusion height and the diffusion layer thickness, respectively. For very fast processes, when $j_0/j_L \gg 1$, i.e., if $f_c \approx f_a$ but $f_c > f_a$, (61) becomes:

$$\eta_{cr} = \frac{RT}{nF} \frac{j_L}{j_0} \left(\frac{\delta}{h}\right)^{\gamma} \tag{65}$$

meaning that in the case of Ohmic-controlled reactions, dendritic growth can be expected at very low overpotentials, or better to say, if $j_0 \to \infty$, instantaneous dendritic growth is possible at all overpotentials if only mass-transfer limitations are taken into consideration.

In fact, dendrite propagation under such conditions is under diffusion and surface energy control and η_{cr} is then given by:[11,21]

$$\eta_{cr} = \frac{8\sigma V}{nFh}, \tag{66}$$

where σ is the metal surface energy and V is the molar volume of the metal.

Hence, a critical overpotential for initiation dendritic growth is also expected in such cases, being of the order of few millivolts.[21,56]

The initiation of dendritic growth is followed by an increase of the deposition current density, and the overall current density will be larger than the limiting diffusion current on a flat active electrode. Based on the above discussion, the polarization curve equation in the Ohmic-controlled electrodeposition of metals can be determined now by:[9]

$$j = \frac{\kappa\eta}{L} \quad \text{for } 0 \le \eta < j_L\frac{L}{\kappa}, \tag{67a}$$

$$j = j_L \quad \text{for } j_L\frac{L}{\kappa} \le \eta < \eta_{cr} + j_L\frac{L}{\kappa}, \tag{67b}$$

$$j = j_L\theta + (1-\theta)j_0\frac{(f_c - f_a)}{N}\sum_{i=1}^{i=N}\left(\frac{h_i}{\delta}\right)^{\gamma} \quad \text{for } \eta_{cr} \le \eta, \tag{67c}$$

where $N = N(t)$ is the number of dendrites and $\theta = \theta(t) \le 1$, where θ is the coverage of the electrode surface with dendrites.

Equation (67a) describes the linear part of the polarization curves for tin,[57] silver,[7] and lead[58] deposition and (67b) foresees the inflection point in the cases when η_{cr} is low and the resistance of the electrolyte large. Finally, (67c) describes the part of the polarization curve after initiation of dendrite growth.

It is interesting to note that (67c) describes qualitatively the increase of the apparent current density over the value of the limiting diffusion current density after initiation of dendritic growth, since the quantitative treatment of the polarization characteristics in the presence of dendrite growth is simply impossible. This is because dendrites can have a variety of unpredictable structures. In this way, the results of Ibl and Schadegg,[59] Diggle et al.,[12] and Popov et al.,[21] as well as the Ohmic-controlled deposition of tin,[57] silver,[7] and lead,[58] could be explained qualitatively.

Thus, instead of a limiting diffusion current density plateau, a curve inflection point or a short inclined plateau can be expected on the polarization curve in Ohmic-controlled electrodeposition of metals, as observed in the case of silver electrodeposition from nitrate solutions. The exchange current density of the silver reaction in nitrate electrolytes is sufficiently large to permit Ohmic-controlled deposition as well as dendritic growth at low overpotentials.[27] After a linear increase of the deposition current density with increasing overpotential, an exponential increase after the inflection point appears, meaning the elimination of mass-transfer limitations due to the initiation of dendritic growth.

The polarization curve for silver electrodeposition from nitrate solution, 0.5 M $AgNO_3$ in 0.2 M HNO_3, onto a graphite electrode is shown in Fig. 15. As shown earlier,[7] the polarization curves for silver deposition from nitrate solution onto a graphite electrode and on graphite covered with a nonporous surface film of silver (hence, on a massive silver electrode) are practically the same. The polarization curve in Fig. 15 is very similar to that in Fig. 7, which means that mass-transfer limitations were decreased or even eliminated. The SEM photomicrographs of the deposit corresponding to the points from Fig. 15 are shown in Fig. 16.

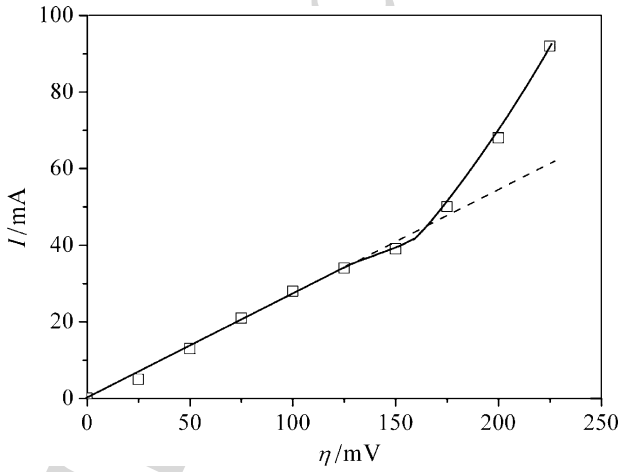

Figure 15. The polarization curve for silver electrodeposition from nitrate solution on a graphite electrode. Reprinted from ref. [9] with permission from Elsevier.

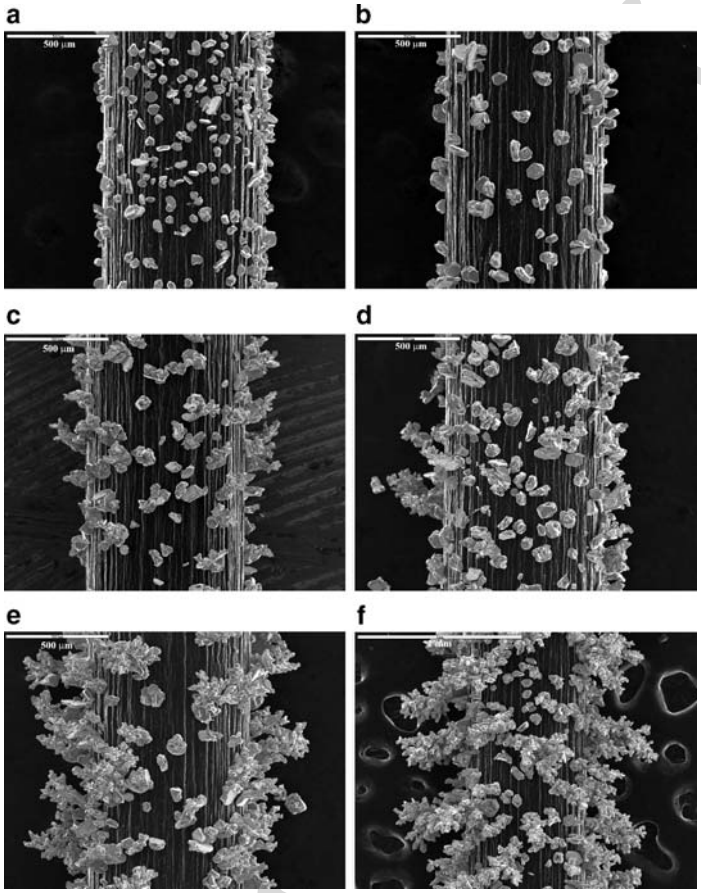

Figure 16. The SEM photomicrographs of the silver deposit obtained on a graphite electrode obtained after the recording of the current at different overpotentials in polarization measurements: (**a**) 100; (**b**) 125; (**c**) 150; (**d**) 175; (**e**) 200; and (**f**) 225 mV. Reprinted from ref. [9] with permission from Elsevier.

It can be seen from Figs. 15 and 16a that at an overpotential of 100 mV, only grains[9] can be seen, which means that the deposition was not under diffusion control. It follows from Figs. 15 and 16b that deposition at an overpotential of 125 mV is still out of diffusion control. At 150 mV, the current density is somewhat lower than that which could be expected from the linear dependence of current

on overpotential. This indicates not only the initiation of diffusion control of the deposition process but also the initiation of dendrite growth, which compensates the mass-transfer limitations, as can be seen from Figs. 15 and 16c. The point corresponding to an overpotential of 150 mV can be considered as the inflection point of the polarization curve in Fig. 15.

At overpotentials larger than 175 mV, the current density is considerably larger than the one expected from the linear dependence of current on overpotential. The formation of dendritic deposits (Fig. 16d–f) confirms that the deposition was dominantly under activation control. Thus, the elimination of mass transport limitations in the Ohmic-controlled electrodeposition of metals is due to the initiation of dendritic growth at overpotentials close to that at which complete diffusion control of the process on the flat part of the electrode surface occurs.

It is necessary to note that the silver deposits shown in Fig. 16d–f are not similar to ideal silver dendrites,[49] but they behave as dendritic ones in regard to their electrochemical properties. Hence, they can be considered as degenerate dendritic deposits.

Occasionally, the needle-like dendrites can also be formed.

On the other hand, due to the overlapping of the nucleation exclusion zones,[7,35,36] deposition on the partially covered graphite electrode is an excellent illustration of the above discussion. Namely, the diffusion layer on the inert electrode partially covered with grains of active metal can be formed and diffusion control established in the same way as on an electrode of massive active metal if the deposition process is characterized by a large j_0/j_L.[7] If dendrites are formed on the grains, their tips enter the bulk solution and overall control of the deposition process becomes activation or mixed controlled.

Naturally, the same effect can be expected if some very fast electrochemical process, other than electrodeposition, occurs on the inert electrode partially covered by dendrites of active catalyst, especially if concentration of reacting ion is low.[60] This could be of great importance for the activation of inert substrates for catalytic purposes.

It is clear that mass-transfer limitation can be avoided if the deposition process is carried out on dendritic electrodes. In order to illustrate this, the electrode shown in Fig. 17 was used. This is a dendrite electrode. It was obtained by deposition of copper on the tip of a copper wire at an overpotential of 650 mV during 20 min from 0.15 M $CuSO_4$ in 0.50 M H_2SO_4.

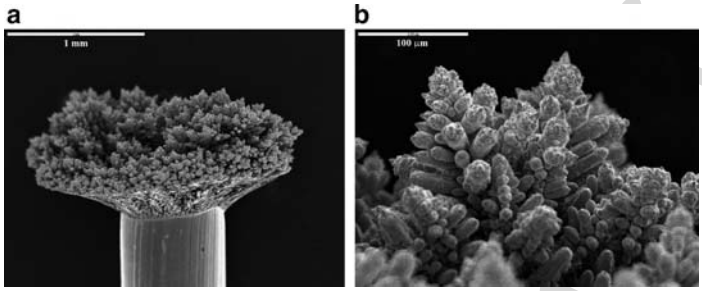

Figure 17. (**a**) The agglomerate of dendrites obtained by deposition of copper on the tip of a copper wire electrode at 650 mV for 20 min; (**b**) the outer limit of the dendritic electrode. Reprinted from ref. [9] with permission from Elsevier.

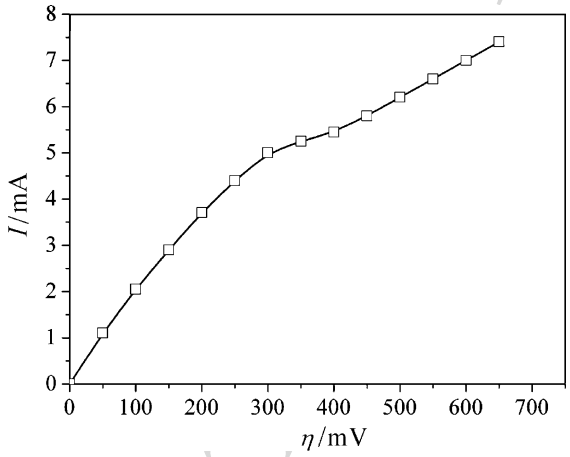

Figure 18. The polarization curve for copper deposition on the electrode from Fig. 17. Reprinted from ref. [9] with permission from Elsevier.

The polarization curve obtained on it from the same solution is shown in Fig. 18.

The shape of polarization curve in Fig. 18 clearly indicates that after the inflection point, activation control becomes dominant.

It also seems that the only way to obtain an ensemble of microelectrodes[16] working independently under activation control is to form an agglomerate of dendrites, the tips of which represent microelectrodes working in the bulk solution outside any diffusion

layer as well as outside the bulk of the agglomerated dendrites. This could be of great importance in the activation of an inert electrode surface by partial covering with dendrites of an active catalyst.

In practice, deposits with high roughness factor and good mechanical resistance are of particular interest. Dendrites have low mechanical resistance and they are unsuitable as electrocatalysts, but the elucidation of the Ohmic-controlled electrodeposition of metals due to the dendritic growth is of a great theoretical importance.

2. Low Level of Coarseness

Any solid metal surface that represents a substrate for electrochemical reactions possesses a certain roughness. The roughness factor is determined as the ratio of atomic scale real area to the geometrically measured apparent one.[61] In addition, it may appear coarse or smooth, and this is not necessarily related to the roughness. It is the level of coarseness that determines the appearance of the metal surface, while even with considerable roughness, if below the visual level, the surface may appear smooth. It is convenient to define the surface coarseness as the difference in thickness of the metal at the highest and lowest point above a reference plane facing the solution. Figure 19 show cases of surfaces with (a) equal roughness and profoundly different coarseness and (b) vice versa.[62]

The apparent surface of polycrystals, measured geometrically, is often two to three times smaller than the real area, because the latter is relatively rough – even if its hills and valleys are invisible to unaided sight. Because various metals and different samples of the same metal may have different roughness factor and because the velocity of an electrode reaction has to be standardized to the real area, the roughness factor has to be determined.[61,62]

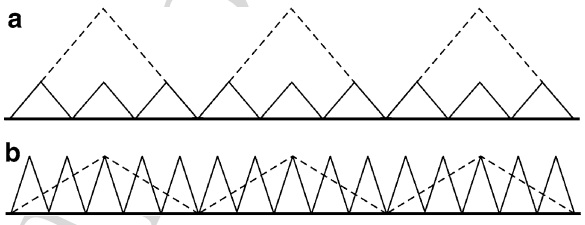

Figure 19. Models of surfaces with: (**a**) equal surface roughness with different coarseness and (**b**) vice versa. Reprinted from ref. [8] with permission of Elsevier.

The standardized values of velocity of electrochemical reactions, expressed by the values of exchange current density standardized to real area, can be compared with each other.

Since both the exchange current density and the limiting diffusion current density are included in the general cathodic polarization curve equation given by (7), it is necessary to standardize them in the same way, hence, to the apparent surface area. In that case, the exchange current density has some effective value, $j_{0,\mathrm{eff}}$, given by (68)

$$j_{0,\mathrm{eff}} = f_{\mathrm{r}} j_0, \tag{68}$$

where f_{r} is the roughness factor and j_0 is the value of the exchange current density standardized to the ideally smooth electrode surface. In similar way, the $j_{0,\mathrm{eff}}$ was defined earlier for the partially covered inert electrode with active catalyst[7] and j on porous electrodes.[63]

Electrocatalysts are produced in different ways, on different substrates, and for different purposes,[10,64–72] but almost in all cases the electrochemical characterization was performed by using the cyclic voltammetry observations. In this way, it was not possible to analyze the effects of the mass-transfer limitations on the polarization characteristics of electrochemical processes. As shown recently,[7,9] the influence of both kinetic parameters and mass-transfer limitations can be taken into account using the exchange current density to the limiting diffusion current density ratio, j_0/j_{L}, for the process under consideration. Increased value of this ratio leads to the decrease of the overpotential at one and the same current density and, hence, to the energy savings.

The basic idea of this section lies in the following facts. In the general polarization curve equation,[61] both exchange and limiting diffusion current densities are standardized to the apparent electrode surface area. Hence, if the electrode surface roughness is increased, the effective value of exchange current density for process under consideration, standardized to the apparent electrode surface area, is also increased. At the same time, if the level of the electrode surface coarseness remains low, the change of the limiting diffusion current density can be neglected. In this way, the value of j_0/j_{L} ratio is increased, what can produce the decrease of overpotential at fixed current density.

At significantly low level of coarseness, the limiting diffusion current does not depend on it, being the same as on the flat

electrode surface. On the contrary, even at significantly low level of coarseness, the surface roughness can be considerably increased as well as the value of the effective exchange current density.

Then, (7) modified with (68) can be used for calculation of the polarization curves for the same electrochemical process at different values of electrode surface roughness at low level of coarseness.

Using (7) and (68), and $f_c = 10^{\eta/120}$ and $f_a = 10^{-\eta/40}$, $j_0/j_L = 0.01$ and 0.1, and $f_r = 1, 2, 5$, and 10, the dependences presented in Fig. 20 are obtained, being valid for copper electrodeposition reaction. The strong decrease of overpotential at the same current densities with increase of the roughness factor of the electrode surface can be seen.

The Ohmic drop is not included in the polarization curve from Fig. 20. The dependences of overpotential at fixed current density on f_r are derived from the diagrams in Fig. 20 and presented in Fig. 21. It can be seen from Fig. 21 that the values of overpotential strongly decrease with increase of f_r.

There are three possibilities for the increase of both the surface roughness and coarseness during electrodeposition of metals. In the activation-controlled electrodeposition the regular crystal grains

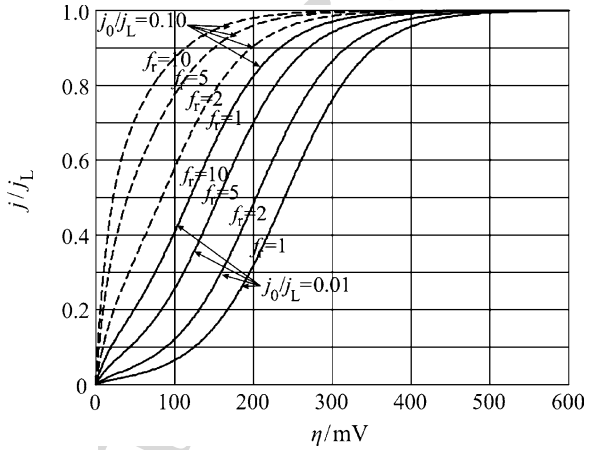

Figure 20. Dependences of $j/j_L - \eta$ calculated from (7) and (68) using $j_0/j_L = 0.1$ and 0.01, $f_r = 1, 2, 5, 10$ and $f_c = 10^{\eta/120}$ and $f_a = 10^{-\eta/40}$. Reprinted from ref. [8] with permission of Elsevier.

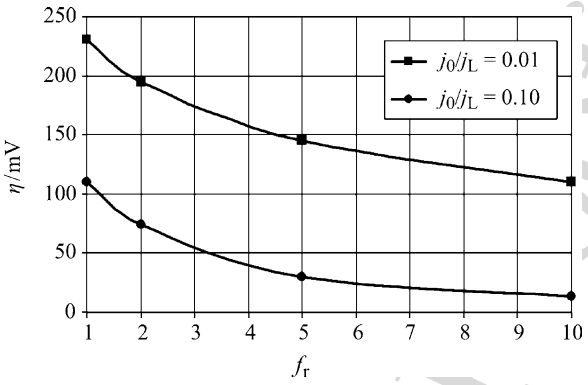

Figure 21. Dependences of overpotential on roughness factor for $j/j_L = 0.5$ and different j_0/j_L ratios. Data derived from Fig. 20. Reprinted from ref. [8] with permission of Elsevier.

grow, in the region of mixed activation–diffusion control there is a nondendritic surface coarseness amplifications, and in the complete diffusion control dendritic deposition appears.[30,48]

It is obvious that in the first case the situation like that from Fig. 19a can be expected, leading to the increase of surface coarseness, i.e., the size of crystal grains, but without considerable change of the surface roughness. In the region of the mixed control, as well as of the diffusion control at overpotentials lower than the overpotential required for dendritic growth initiation, the cauliflower-like forms are mainly formed, and they can be approximated by hemispherical protrusions. Finally, at overpotentials higher than the one required for dendritic growth initiation, dendrites are formed, and they can be approximated by cones. It is easy to show that for $\delta \gg r$, the surface roughness does not depend on the radius of the cauliflower-like particle.[30] A schematic presentation of the top view of the flat surface covered with homogeneously distributed equal hemispherical protrusions and corresponding cross section is presented in Fig. 22.

It is easy to show that roughness factor $f_{r,h}$ in this case is given as

$$f_{r,h} = 1 + \frac{\pi}{4}, \tag{69}$$

being independent on the radius of hemispherical protrusions.

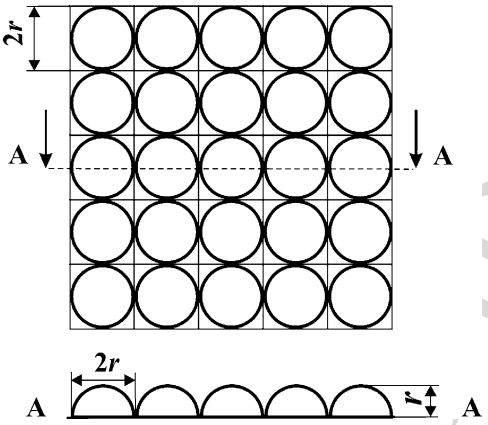

Figure 22. A schematic representation of the top view of the electrode surface modified with equal spherical protrusions and of corresponding cross-section. Reprinted from ref. [8] with permission of Elsevier.

If instead of hemispherical protrusions, the conic ones are used, characterized by radius of base r and the height h, the roughness factor $f_{r,c}$ is given as

$$f_{r,c} = 1 - \frac{\pi}{4} + \frac{\pi}{2r}(h^2 + r^2)^{\frac{1}{2}}, \tag{70}$$

being strongly dependant on the h/r ratio. Corresponding schematic presentation is given in Fig. 23.

Although the above illustration is a qualitative one, it can be concluded by the analysis of (69) and (70) that the roughness factor during nondendritic surface roughness amplification can be enlarged about two times. On the other hand, during dendritic growth, amplification can be many times larger than in the nondendritic one.

Hence, the activation overpotential can be considerably decreased by appropriate preparation of electrode surface morphology, especially by formation of disperse deposits at low level of coarseness. Obviously, the roughness factor can be increased many times in real situations. It is well known that the surface morphology exerts a marked influence on the electrocatalytic activity of an electrode.[73] At a microscopic level, the existence of pores, crevices, microcavities, etc. favors the increase of the electrodic surface area, though

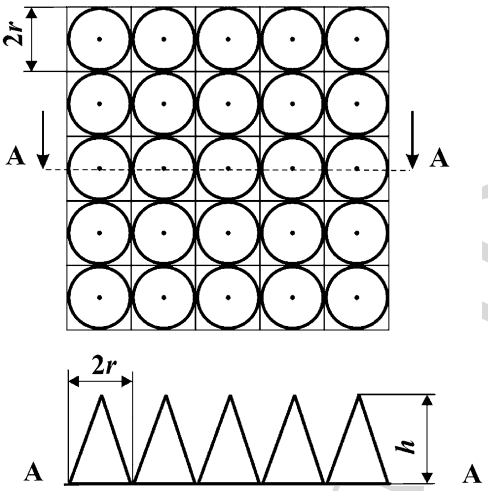

Figure 23. A schematic representation of the top view of the electrode surface modified with equal conical protrusions and of corresponding cross-section. Reprinted from ref. [8] with permission of Elsevier.

mass transfer, Ohmic, and bubble overvoltages prevent the rates of electrochemical reactions from increasing proportionally.[10] An example is the Raney-Nickel electrode used as cathodic material for the hydrogen evolution reaction, for which it has been found that in certain cases only 1.5% of the available area is used.[74] In order to avoid the discrepancy between the overall electrode surface and the part of it at which the electrochemical process occurs in prolonged electrolysis, the procedure of the determination of the effective value of roughness factor has been developed.[75] This is done by determining the exchange current densities from stationary polarization curves. The roughness factors were determined as ratios of the values of exchange current densities on different substrates and on the reference one. In this way, the differences in surface areas taking place in determination of roughness factor and in prolonged electrolysis process are avoided.

The copper deposit obtained by electrodeposition at an overpotential of 300 mV during 2 min at copper cylindrical electrode is shown in Fig. 24a. Copper deposits electrodeposited at overpotentials of 550 and 650 mV on the copper electrode presented in Fig. 24a

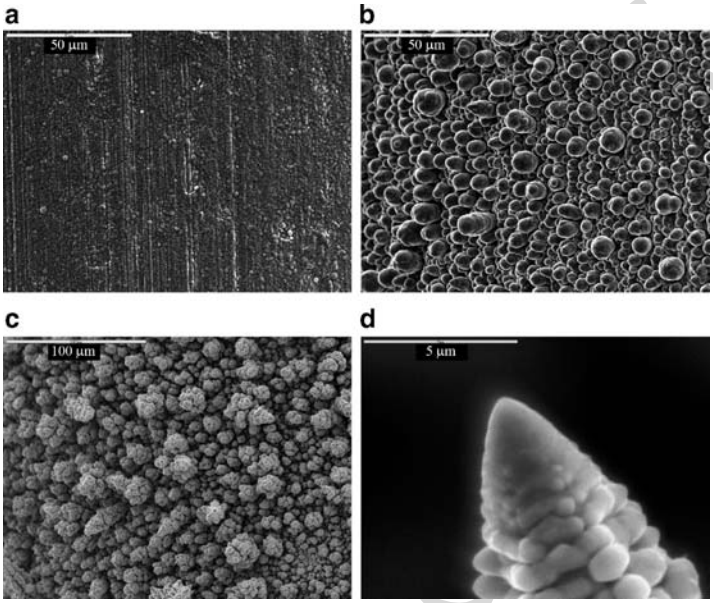

Figure 24. (**a**) The copper deposit electrodeposited at an overpotential of 300 mV during 2 min on the cylindrical copper electrode; and copper deposits electrodeposited with 5.0 mA h cm^{-2} on the copper substrate from (**a**) at overpotentials of: (**b**) 550 mV and (**c**) 650 mV; (**d**) the top of copper dendrite electrodeposited at an overpotential of 650 mV with a deposition time of 32 min. Reprinted from ref.[8] with permission of Elsevier.

with a quantity of electricity of 5.0 mA h cm^{-2} are shown in Fig. 24b and c, respectively.

The polarization curves recorded on the cylindrical platinum electrodes treated in the same way as the cylindrical copper electrodes in Fig. 24 are shown in Fig. 25. There is not any difference between polarization curves obtained on the copper and platinum substrates.

The mutual position of the polarization curves from Fig. 25 indicates that the exchange current density corresponding to the substrate from Fig. 24c is considerably larger than other ones. The conclusion can be derived by the comparison of Figs. 20 and 25, because the Ohmic voltage drop in the polarization curves from Fig. 25 does

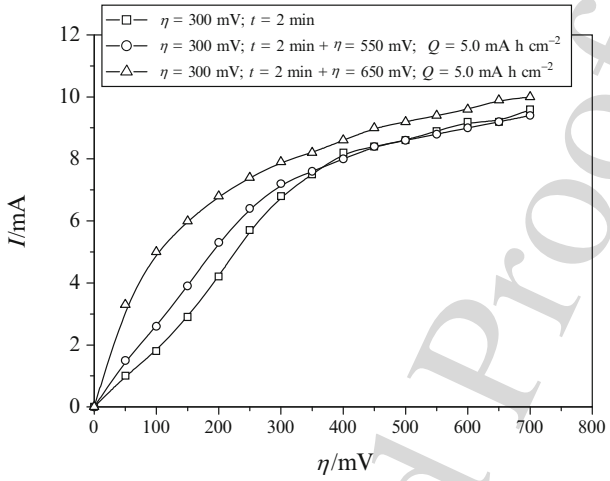

Figure 25. Polarization curves for copper electrodeposition on the cylindrical platinum electrodes treated by copper electrodeposition under the same conditions shown in Fig. 24a–c. Reprinted from ref. [8] with permission of Elsevier.

not affect the mutual position of polarization curves in which the Ohmic voltage drop is not included.[9]

On the other hand, as was shown recently,[75] the value of j_0 can be estimated using j_L value extracted from the polarization curve and known value of the cathodic Tafel slope b_c by (71)

$$j_0 = \frac{j_L}{10^{\frac{\eta_{1/2}}{b_c}}} \tag{71}$$

if the Ohmic voltage drop can be neglected, where $\eta_{1/2}$ is the value of overpotential corresponding to the half of limiting diffusion current density value. For electrode surfaces presented in Fig. 24a–c, using $b_c = 120\,\mathrm{mV\,dec^{-1}}$ and j_L from polarization curves presented in Fig. 25, exchange current density values can be estimated as $j_0 = 0.14$, 0.27, and $1.8\,\mathrm{mA\,cm^{-2}}$, respectively. This method can be applied here because the Ohmic voltage drop can be neglected for the electrode whose surface is presented in Fig. 24a. Increasing surface roughness decreases the overpotential at fixed value of apparent current density and the contribution of Ohmic voltage drop

to the measured overpotential increases. Because of this, the value of j_0 calculated by (71) can become lower than the real value, and, hence, it can be used in this qualitative discussion.

Equation (68) can be rewritten in the form

$$f_r = \frac{j_{0,\mathrm{eff}}}{j_0}. \tag{72}$$

Assuming that j_0 corresponds to the substrate from Fig. 24a and that exchange current density values corresponding to the other substrates are the effective values, roughness factors of 1.9 and 13 for substrates shown in Fig. 24b, c, respectively, are obtained. The copper deposit formed by the nondendritic surface coarseness amplification at an overpotential of 550 mV (Fig. 24b) is well described by Fig. 22, and calculated value of 1.9 is close to the one predicted by (69). The copper deposit obtained at an overpotential of 650 mV (Fig. 24c) represents the precursors of dendrites which can be described, more or less successfully, by cones from Fig. 23. It is necessary to note that different forms on such surface are formed, from the dendritic precursor to completely formed dendrite. Also, it can be clearly seen from Fig. 24d that the top of the dendrite formed at an overpotential of 650 mV was like a cone. Anyway, inhomogeneous surface with different levels of coarseness was obtained, regardless of the limiting diffusion current density value, which was not considerably increased. The roughness factor for this electrode, calculated by (72), is $f_r = 13$, being considerably larger than the previous one.

The formation of the smaller (and less different to each other) dendrites could be obtained by the increase of deposition overpotential. Unfortunately, the increased overpotential produces the hydrogen evolution in this system and the formation of degenerate dendrites and honeycomb-like deposits.[76,77] Nevertheless, the dendritic growth in this system at larger overpotentials is possible by the application of appropriate square-wave pulsating overpotential (PO) regime. For example, the well-developed dendrites were formed with amplitude overpotential of 1,000 mV, deposition pulse of 10 ms, and pause of 100 ms (the pause to pulse ratio: 10) (Fig. 26a). They can be well approximated by the cones shown in Fig. 23. Also, superficial holes due to attached hydrogen bubbles were formed between these dendrites, as can be seen from ref. [78]

AQ5 The precursors of dendrites, like a cone, were also formed by the square-wave PO with the same amplitude overpotential and the

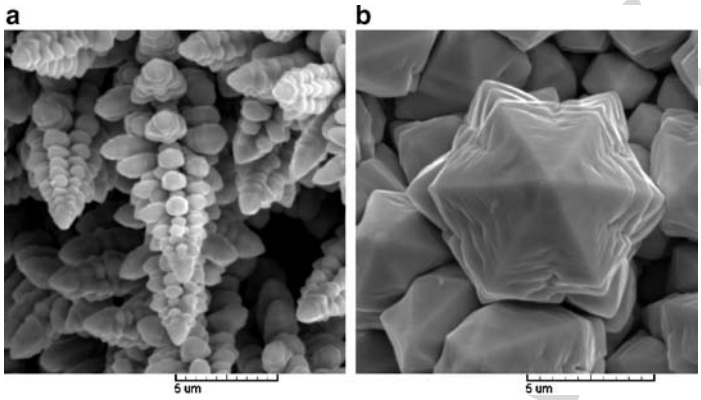

Figure 26. (**a**) The copper dendrites formed by the pulsating overpotential (PO) regime: deposition pulse of 10 ms, pause duration of 100 ms; deposition time: 18 min; (**b**) The precursor of copper dendrite obtained by PO regime: deposition pulse of 1 ms, pause duration of 10 ms; deposition time: 24 min. In both cases amplitude overpotential used was 1,000 mV. Reprinted from ref. [8] with permission of Elsevier.

pause to pulse ratio of 10, but by applying deposition pulse of 1 ms and pause of 10 ms (Fig. 26b). In this square-wave PO, hydrogen evolution was avoided.[79]

The polarization curves for copper deposition on the electrodes whose surfaces are shown in Fig. 24a and 26a are given in Fig. 27. It is obvious that the noticeable increase of the exchange current density attained by the application of the PO regime ($j_{0,\mathrm{eff}} = 3.3\,\mathrm{mA\,cm^{-2}}$; $f_r = 23.5$) is followed by the minimal increase of limiting diffusion current density, relative to the one corresponding to the substrate from Fig. 24a.

The same polarization characteristics exhibit the platinum electrode modified with copper dendrites formed by the use of the PO regime described in caption of Fig. 26a. It can be seen from Fig. 27 that the process on the electrode with increased surface roughness takes place at considerably lower overpotential than on the smoother one.

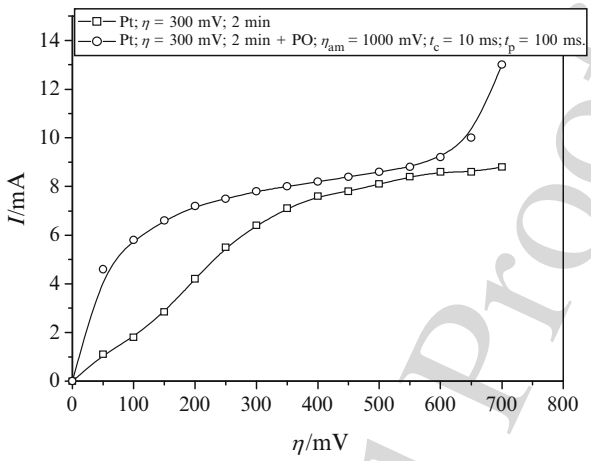

Figure 27. Polarization curves for copper electrodeposition on the substrates from Figs. 24a and 26a. Reprinted from ref.[8] with permission of Elsevier.

V. APPLIED ASPECTS

The discussion presented in this chapter is new, and it is difficult to relate it to some current applications. However, some important conclusions and recommendations can be suggested from this chapter.

First, it is possible to produce the copper dendrites by the PO deposition at the overpotential amplitude at which in a constant current regime the honeycomb-like deposits are formed. The dendrites produced by the PO regime were very small but well developed, increasing considerably the electrode surface roughness even at low level of coarseness. In other words, the apparent exchange current density of the electrochemical process occurring on such electrode can be increased for more than 20 times in comparison with one occurring at the smooth electrode surface. This result suggests that important saving in energy can be achieved. A nondendritic surface roughening does not produce significant increase in the exchange current density.

Second, as it was recently shown,[2,9] the ratio of the exchange current density and the limiting diffusion current density, j_0/j_L, determines the polarization characteristics of an electrochemical processes. Increased value of this ratio leads to a decrease of the

activation overpotential at the same applied current density. If $j_0/j_L \geq 100$, the process becomes Ohmic controlled. In this situation, not only the activation overpotential is lost, but also the diffusion overpotential at current densities lower than the limiting diffusion is lost. This means that the electrochemical process on the smooth electrode surface characterized by the value of $j_0/j_L < 5$ can be transformed to Ohmic-controlled one on the electrode surface from Fig. 26a.

As already shown, for selected set of operating conditions, the $j_{0,eff}/j_L$ value can be only altered by a change of the electrode surface roughness. The j_0/j_L ratio for the electrode whose surface is presented in Fig. 24a is 0.018 and for that presented in Fig. 26a is 0.40. It can be seen from Fig. 27 that at same current densities, belonging to the operating region of current density, about 70% of overpotential, hence energy, can be saved by using electrode with larger surface roughness at approximately the same surface coarseness. As explained earlier, the Ohmic voltage drop is neglected in this case.

Copper shows a high activity for nitrate ion reduction[80,81] as well as for a reaction in which nitrate is reduced to ammonia with a high yield from aqueous acidic perchlorate and sulphate solutions.[82] In the future, the comparison of the polarization characteristics of the mentioned reactions on a smooth electrode surface and on the rough one at low level of coarseness should be investigated in detail.

The electrode surface roughness at low level of coarseness can be increased in some different ways other than dendrites (spongy-like deposit,[33] honeycomb-like structure,[76,77] pyramid-like deposit,[83] etc.) on the microscale. The properties of electrodeposits on nanoscale should be also taken into consideration.[84,85] Further investigation will show which one of them is the best for this purpose. This chapter is written in order to initiate it.

VI. CONCLUSIONS

A completely new approach to the analysis of experimental data is introduced by the use of the complete polarization curve equation and by the method of digital simulation. It was possible in this way to elucidate the polarization behavior of the partially covered inert

electrodes, the essence of the Ohmic-controlled electrodeposition of metals, and the electrocatalytic properties of disperse electrodeposits formed at low level of the electrode coarseness.

Doubtless, the main contribution of this chapter is (57), which correlates the quantity of catalyst required for complete activation of inert electrode with size and density of hemispherical active grain and parameters of electrochemical process taking place on them.

ACKNOWLEDGMENTS

The work was supported by the Ministry of Science and Technological Development of the Republic of Serbia under the research projects: "Deposition of ultrafine powders of metals and alloys and nanostructured surfaces by electrochemical techniques" (No. 142032G) and "Modification of metal and nonmetal materials by electroconductive polymer for application in new technologies" (No. 142044).

REFERENCES

[1]S. Trasatti, "*Electrocatalysis in Water Electrolysis*", *Book of Abstracts, 1st Regional Symposium on Electrochemistry of South-East Europe*, Rovinj, Croatia (2008) 1.

[2]Y. Takasu, T. Kawaguchi, W. Sugimoto, and Y. Murakami, *Electrochim. Acta* **48** (2003) 3861.

[3]Y. Takasu, N. Ohashi, X. -G. Zhang, Y. Murakami, H. Minagawa, S. Sato, and K. Yahikozawa, *Electrochim. Acta* **41** (1996) 2595.

[4]N. Pron'kin, O. A. Petrii, G. A. Tsirlina, and D. J. Schiffrin, *J. Electroanal. Chem.* **480** (2000) 112.

[5]L. Nzoghe-Mendome, A. Aloufy, J. Ebothe, M. El Messiry, and D. Hui, *J. Cryst. Growth* **311** (2009) 1206.

[6]J. O'M. Bockris, A. K. N. Reddy, and M. Gamboa-Aldeco, *Modern Electrochemistry 2 A*, 2nd edition, Kluwer/Plenum, New York (2000) 1361.

[7]K. I. Popov, P. M. Živković, and B. N. Grgur, *Electrochim. Acta* **52** (2007) 4696.

AQ6 [8]K. I. Popov, N. D. Nikolić, P. M. Živković, and G. Branković, *Electrochim. Acta*, in press, doi: 10.1016/j.electacta.2009.10.085.

[9]K. I. Popov, P. M. Živković, S. B. Krstić, and N. D. Nikolić, *Electrochim. Acta* **54** (2009) 2924.

[10]C. A. Marozzi and A. C. Chialvo, *Electrochim. Acta* **45** (2000) 2111.

[11]J. L. Barton and J. O'M. Bockris, *Proc. R. Soc. A* **268** (1962) 485.

[12]J. W. Diggle, A. R. Despić, and J. O'M Bockris, *J. Electrochem. Soc.* **116** (1969) 1503.

[13]A. R. Despić, J. W. Diggle, and J. O'M Bockris, *J. Electrochem. Soc*. **116** (1969) 507.
[14]J. O'M. Bockris and A. K. N. Reddy, *Modern Electrochemistry 2 B*, 2nd edition, Kluwer/Plenum, New York (2000) 1811.
[15]B. Scharifker and G. Hills, *Electrochim. Acta* **28** (1983) 879.
[16]E. Gilleadi, *Electrode Kinetics*, VCH Publishers, New York (1993) 443.
[17]P. Stonehart and D. Wheeler, "*Phosphoric Acid Fuel Cells (PAFCs) for vehicles; Electrocatalyst Crystalite Design, Carbon Support, and Matrix Materials Challenges*" in *Modern Aspects of Electrochemistry*, Vol. 38, Ed. by B. E. Conway, Kluwer/Plenum, New York (2005) Chapter 4, 385.
[18]J. O'M. Bockris, A. K. N. Reddy, and M. Gamboa-Aldeco, *Modern Electrochemistry 2 A*, 2nd edition, Kluwer/Plenum, New York (2000) 1248.
[19]K. I. Popov, S. S. Djokić, and B.N. Grgur, *Fundamental Aspects of Electrometallurgy*, Kluwer/Plenum, New York (2002) Chapter 3, 14.
[20]K. I. Popov, N. V. Krstajić, and M. I. Čekerevac, "*The Mechanism of Formation of Coarse and Disperse Electrodeposits*" in Ed. by R. E. White, B. E. Conway, and J. O'M. Bockris, *Modern Aspects of Electrochemistry*, Vol. 30, Plenum, New York (1996) Chapter 3, 262.
[21]K. I. Popov, M. D. Maksimović, J. D. Trnjavčev, and M. G. Pavlović, *J. Appl. Electrochem*. **11** (1981) 239.
[22]J. S. Newman, *Electrochemical Systems*, Prentice-Hall, Engelwood Cliffs, NJ (1973) 177.
[23]M. N. Dešić, M. M. Popović, M. D. Obradović, Lj. M. Vračar, and B. N. Grgur, *J. Serb. Chem. Soc*. **70** (2005) 231.
[24]P. M. Živković, B. N. Grgur, and K. I. Popov, *J. Serb. Chem. Soc*. **73** (2008) 227.
[25]J. O'M. Bockris, A. K. N. Reddy, and M. Gamboa-Aldeco, *Modern Electrochemistry 2 A*, 2nd edition, Kluwer/Plenum, New York (2000) 1107.
[26]K. I. Popov, S. S. Djokić, and B.N. Grgur, *Fundamental Aspects of Electrometallurgy*, Kluwer/Plenum, New York (2002) Chapter 3, 87, 88.
[27]P. B. Price and D. A. Vermilyea, *J. Chem. Phys*. **28** (1958) 720.
[28]W. Lorenz, *Z. Electrochem*. **58** (1954) 912.
[29]B. E. Mattsson and J. O'M. Bockris, *Trans. Faraday Soc*. **55** (1959) 1586.
[30]K. I. Popov, S. S. Djoki, and B.N. Grgur, *Fundamental Aspects of Electrometallurgy*, Kluwer/Plenum, New York (2002) Chapter 3, 56.
[31]K. I. Popov, V. Radmilović, B. N. Grgur, and M. G. Pavlović, *J. Serb. Chem. Soc*. **59** (1994) 47.
[32]K. I. Popov, N. V. Krstajić, S. R. Popov, and M. I. Čekerevac, *J. Appl. Electrochem*. **16** (1986) 771.
[33]K. I. Popov and N. V. Krstajić, *J. Appl. Electrochem*. **13** (1983) 775.
[34]K. I. Popov, N. V. Krstajić, and S. R. Popov, *J. Appl. Electrochem*. **15** (1985) 151.
[35]I. Markov, A. Boynov, and S. Toshev, *Electrochim. Acta* **18** (1973) 377.
[36]S. Štrbac, Z. Rakočević, K. I. Popov, M. G. Pavlović, and R. Petrović, *J. Serb. Chem. Soc*. **64** (1999) 483.
[37]A. Dimitrov, S. Hadži-Jordanov, K. I. Popov, and M. G. Pavlović, *J. Appl. Electrochem*. **28** (1998) 791.
[38]V. Radmilović, K. I. Popov, M. G. Pavlović, A. Dimitrov, and S. Hadži-Jordanov, *J. Solid State Electrochem*. **2** (1998) 162.
[39]K. I. Popov, B. N. Grgur, E. R. Stoiljković, M. G. Pavlović, and N. D. Nikolić, *J. Serb. Chem. Soc*. **62** (1997) 433.
[40]G. D. Adžić, A. R. Despić, and D. M. Dražić, *J. Electroanal. Chem*. **220** (1988) 169.
[41]G. D. Adžić, A. R. Despić, and D. M. Dražić, *J. Electroanal. Chem*. **241** (1988) 353.

[42]N. Ya. Kovarskii and T. A. Arzhanova, *Elektrokhimiya* **22** (1986) 452.
[43]M. L. Avramov Ivić, S. D. Petrović, P. M. Živković, N. D. Nikolić, and K. I. Popov, *J. Electroanal. Chem*. **549** (2003) 129.
[44]K. I. Popov, M. G. Pavlović, Lj. J. Pavlović, M. I. Čekerevac, and G. Ž. Remović, *Surf. Coat. Technol*. **34** (1988) 355.
[45]K. I. Popov, N. V. Krstajić, Z. D. Jerotijević, and S. P. Marinković, *Surf. Technol*. **26** (1985) 185.
[46]K. J. Vetter, Electrochemical kinetics, Khimiya, Moskva, 1967, p. 699, Section 162 C, and references therein (in Russian).
[47]K. I. Popov, N. V. Krstajić, and S. R. Popov, *Surf. Technol*. **20** (1983) 203.
[48]K. I. Popov, S. S. Djokić, and B.N. Grgur, *Fundamental Aspects of Electrometallurgy*, Kluwer/Plenum, New York (2002) Chapter 3, 78.
[49]G. Wranglen, *Electrochim. Acta* **2** (1960) 130.
[50]A. R. Despić and K. I. Popov, "*Transport controlled Deposition and Dissolution of Metals*", in Ed. by B. E. Conway and J. O'M. Bockris, *Modern Aspects of Electrochemistry*, Vol. 7, Plenum, New York (1972) Chapter 4, 241.
[51]I. N. Justinijanović and A. R. Despić, *Electrochim. Acta* **18** (1973) 709.
[52]K. I. Popov, M. I. Čekerevac, and Lj. M. Nikolić, *Surf. Coat. Technol*. **34** (1988) 219.
[53]K. I. Popov and M. I. Čekerevac, *Surf. Coat. Technol*. **37** (1989) 435.
[54]I. M. Epstein, *Elektrokhimiya* **2** (1966) 734.
[55]K. I. Popov, N. V. Krstajić, and M. I. Čekerevac, "*The Mechanism of Formation of Coarse and Disperse Electrodeposits*" in Ed. by R. E. White, B. E. Conway, and J. O'M. Bockris, *Modern Aspects of Electrochemistry*, Vol. 30, Plenum, New York (1996) Chapter 3, 294.
[56]K. I. Popov, N. V. Krstajić, and M. I. Čekerevac, "*The Mechanism of Formation of Coarse and Disperse Electrodeposits*" in Ed. by R. E. White, B. E. Conway, and J. O'M. Bockris, *Modern Aspects of Electrochemistry*, Vol. 30, Plenum, New York (1996) Chapter 3, 308.
[57]S. Meibhur, E. Yeager, A. Kozawa, and F. Hovorka, *J. Electrochem. Soc*. **110** (1963) 190.
[58]K. I. Popov, M. G. Pavlović, E. R. Stojilković, and Z. Ž. Stevanović, *Hydrometallurgy* **46** (1997) 321.
[59]N. Ibl and K. Schadegg, *J. Electrochem. Soc*. **114** (1967) 54.
[60]P. M. Živković, N. D. Nikolić, M. Gvozdenović, and K. I. Popov, *J. Serb. Chem. Soc*. **74** (2009) 291.
[61]J. O'M. Bockris, A. K. N. Reddy, and M. Gamboa-Aldeco, *Modern Electrochemistry 2 A*, 2nd edition, Kluwer/Plenum, New York (2000) 1095.
[62]A. R. Despić and K. I. Popov, "*Transport controlled Deposition and Dissolution of Metals*", in Ed. by B. E. Conway and J. O'M. Bockris, *Modern Aspects of Electrochemistry*, Vol. 7, Plenum, New York (1972) Chapter 4, 204.
[63]Yu. Chizmadzhev and Yu. G. Chirkov, "*Porous Electrodes*", in Ed. by E. Yeager, J. O'M. Bockris, B. E. Conway, and S. Sarangapani, *Comprehensive Treatise of Electrochemistry*, Vol. 6, Plenum, New York and London (1983) Chapter , 317.
[64]M. V. Ananth, V. V. Giridhar, and K. Renuga, *Int. J. Hydrogen Energ*. **34** (2009) 658.
[65]C. A. Marozzi and A. C. Chialvo, *Electrochim. Acta* **46** (2001) 861.
[66]L. Zhou, Y. F. Cheng, and M. Amrein, *J. Power Sources* **177** (2008) 50.
[67]M. Imamura, T. Haruyama, E. Kobatake, Y. Ikariyama, and M. Aizawa, *Sens. Actuators B* **24–25** (1995) 113.
[68]H. -K. Seo, D. -J. Park, and J. -Y. Park, *Thin Solid Films* **516** (2008) 5227.
[69]I. G. Casella, *Electrochim. Acta* **54** (2009) 3866.

[70]S. A. S. Machado, J. Tiengo, P. de Lima Neto, and L. A. Avaca, *Electrochim. Acta* **39** (1994) 1757.
[71]L. Li, F. Ye, L. Chen, T. Wang, J. Li, and Z. Wang, *J. Power Sources* **186** (2009) 320.
[72]V. Diaz, S. Real, E. Teliz, C. F. Zinola, and M. E. Martins, *Int. J. Hydrogen Energ*. **34** (2009) 3519.
[73]D. Pletcher, *J. Appl. Electrochem*. **14** (1984) 403.
[74]K. Lohrberg and P. Kohl, *Electrochim. Acta* **29** (1984) 1557.
[75]N. D. Nikolić, Lj. J. Pavlović, M. G. Pavlović, and K. I. Popov, *J. Serb. Chem. Soc*. **72** (2007) 1369.
[76]N. D. Nikolić, K. I. Popov, Lj. J. Pavlović, and M. G. Pavlović, *J. Electroanal. Chem*. **588** (2006) 88.
[77]N. D. Nikolić, Lj. J. Pavlović, M. G. Pavlović, and K. I. Popov, *Electrochim. Acta* **52** (2007) 8096.
[78]N. D. Nikolić, G. Branković, V. M. Maksimović, M. G. Pavlović, and K. I. Popov, *J. Solid State Electrochem*. **14** (2010) 331.
[79]N. D. Nikolić, G. Branković, V. M. Maksimović, M. G. Pavlović, and K. I. Popov, *J. Electroanal. Chem*. **635** (2009) 111.
[80]G. E. Dima, A. C. A. de Vooys, and M. T. M. Koper, *J. Electroanal. Chem*. **554–555** (2003) 15.
[81]W. -Y. Ko, W. -H. Chen, C. -Y. Cheng, and K. -J. Lin, *Sens. Actuators B* **137** (2009) 437.
[82]D. Pletcher and Z. Poorbedi, *Electrochim. Acta* **24** (1979) 1253.
[83]K. I. Popov, T. M. Kostić, N. D. Nikolić, E. R. Stojilković, and M. G. Pavlović, *J. Electroanal. Chem*. **464** (1999) 245.
[84]A. J. Arvia and R. C. Salvarezza, *Electrochim. Acta* **39** (1994) 1481.
[85]W. -Y. Ko, W. -H. Chen, S. -D. Tzeng, S. Gwo, and K. -J. Lin, *Chem. Mater*. **18** (2006) 6097.